ORTHOGONAL SIGNAL ALIGNMENT WITH VARIABLE RATE AND POWER IN MIMO Y CHANNELS

by

Xueying Yuan

Submitted in partial fulfillment of the requirements
for the degree of Master of Applied Science

at

Dalhousie University
Halifax, Nova Scotia
June 2016

To My Parents and Family

Table of Contents

List of Tables

List of Figures

Abstract

The multiple-input multiple-output (MIMO) Y channel employs signal alignment (SA) to improve spectral efficiency of wireless networks. In this system of three nodes exchanging data via the relay, cooperation of terminals allows the data transfer of six messages in two phases, medium access control (MAC) and broadcast, each taking one time slot thus achieving up to three times the rate of the conventional relaying system without SA. The antenna configuration in the original MIMO Y channel imposes limitations on controlling the minimum distance between signaling points representing network coded messages and this affects symbol error rate performance. To mitigate this problem, this thesis proposes to add one redundant antenna at every user and designs corresponding precoding vectors to obtain flexibility in the selection of orthogonal signaling dimensions and to simplify decoding at the relay. Additionally, the thesis develops adaptive power allocation and bit loading to optimize the system performance.

List of Abbreviations and Symbols Used

2D	2-dimensional
3D	3-dimensional
AF	amplify-and-forward
ANC	analog network coding
AWGN	additive white Gaussian noise
BC	broadcast
BER	bit error rate
BPSK	binary phase shift keying
CSI	channel state information
DF	decode-and-forward
EM	electromagnetic
IA	interference alignment
MA	margin-adaptive
MAC	medium access control
MAI	multiple access interference
MATLAB®	mathematical laboratory
MIMO	multiple-input multiple-output
ML	maximum likelihood
MMSE	minimum mean square error
NC	network coding
OFDM	orthogonal frequency division multiplexing
PAM	pulse amplitude modulation
PNC	physical network coding
PSK	phase shift keying
QAM	quadrature amplitude modulation
QPSK	quadrature phase shift keying
RA	rate-adaptive
SA	signal alignment

SER	symbol error rate
SNR	signal-to-noise ratio
TDMA	time division multiple access
TS(s)	time slot(s)
TWRC	two-way relay channel
XOR	exclusive or
ZF	zero-forcing

Acknowledgements

First, I would like to give my thanks to my supervisor Dr.Ilow, who has taught me many things. I also would like to thank all colleagues in my research group: Aasem Alyahya, Rashed Alsakarnah, Fadhel Alhumaidi, Md Sabbir Hussain, Mahdi Attaran, Zichao Zhou and Hui Xiong for their generous help. Finally, I'd like to thank my family and friends for their support and understanding.

Chapter 1

Introduction

Recent developments in wireless communication system designs are driven by the goal of achieving high utilization of radio resources like spectrum and power. With the ever growing demands for more sophisticated wireless services, the ultimate objective is to support an increased number of users and higher data rates. To achieve this goal, several new approaches have been proposed recently with the cooperation of terminals, signal alignment (SA) and more advanced relaying strategies offering some of promising breakthroughs. In this thesis, we focus on using SA in cooperative relay networks with multiple-input multiple-output (MIMO) terminals, where multiple transmissions take place simultaneously over a common broadcast communication medium. Specifically, in a multi-way communication network with three nodes exchanging messages with each another through a relay, called the Y channel, this thesis designs a signal processing scheme to obtain the flexibility in the selection of orthogonal signaling dimensions and to simplify the decoding at the relay.

Because of the broadcast nature of the wireless medium, when multiple signals are transmitted at the same time and frequency to increase bandwidth utilization, multiple access interference (MAI) is inevitably introduced. The recently proposed interference alignment (IA) has mitigated the problems of MAI presented in the conventional medium access schemes [1] by aligning signals in time, frequency or space. Specifically, IA confines MAI to a small signal dimension subspace and leaves the majority of signaling dimensions for desired signals, which allows for efficient utilization of bandwidth. On the other hand, SA utilizes the concept of signal space management from IA, and intends to align two desired signals from two users as a whole to perform detection and encoding at the relay.

In the MIMO Y channel system, deploying SA and network coding, the data exchange of six messages among three users is completed in two time slots (TSs), which significantly enhances the throughput of the network over time division multiple

access (TDMA). In the first TS, called the multiple access control (MAC) phase, three users send all messages simultaneously to the relay, and in the second TS, called the broadcast (BC) phase, the relay transmits messages to users also on a single MIMO channel access [2]. In a MIMO Y channel, all dimensions in a signal space at the relay are exploited for transmitting network coded signal representations of three aligned messages with the latter corresponding to network coded symbols exchanged between a pair of users. In the MIMO Y channel scheme, the signal alignment is accomplished via precoding vectors at the user sides in the MAC phase and the relay in the BC phase. The relay in the MAC and the BC phases calls for working with three receive/transmit antennas, while the user terminals can operate with the minimum of two antennas. The antenna configuration where the relay is equipped with three antennas and each user is equipped with two antennas is called the original MIMO Y channel. This system imposes limitations on controlling the minimum distance between signaling points representing network coded messages, and this affects symbol error rate performance.

To mitigate this problem, this thesis adds one redundant antenna at every user and designs corresponding precoding vectors to obtain the flexibility in the selection of orthogonal signaling dimensions and to simplify decoding at the relay. The thesis proposes different designs and optimization of precoding vectors to improve the bit error rate (BER) performance over the original scheme. Specifically, we apply power allocation to distribute energy among the users based on their channel conditions. In addition, iterative optimization of signaling dimensions and time scheduling of transmissions according to channel states are employed to further improve the BER performance. We also propose the deployment of quadrature amplitude modulation (QAM) in the MIMO Y channel and present adaptive deployment of QAM through bit loading techniques.

The remainder of this chapter is organized as follows: in sections 1.1, 1.2 1.3 and 1.4, we present the building blocks related to our research in more detail, namely, (i) network coding, (ii) SA, (iii) the original MIMO Y channel, and (iv) the bit loading techniques. Section 1.5 describes the thesis objectives, while Section 1.6 presents the organization of the whole thesis.

1.1 Wireless Network Coding

In wireless networks, there are two kinds of relays: amplify-and-forward (AF) and decode-and-forward (DF) [3]. Relays in AF mode just amplify the received signal and retransmit it, while relays in DF mode decode the received signal to reduce noise effects, and then transmit the re-encoded signal. In cooperative communications considered in this thesis, DF relays are required in order to process the received data.

Network coding (NC) is a technique where signals sent from terminals are mixed together at relays and the relays transmit the combined signals to terminals, which improves the network throughput. Although NC was initially proposed in the field of wire-line networks [4], there has been growing interest in the application of NC in wireless communications, because the broadcast nature of the wireless medium brings greater efficiency in increasing the system capacity than in wire-line systems.

On the other hand, if the relay can broadcast mixed messages, it can also receive mixed messages to further improve the throughput. It is practical because the analog signals sent from terminals are electromagnetic (EM) waves that can be naturally superimposed in the air as one signal. The wireless NC using this scheme is divided into two parts: physical-layer network coding (PNC) [5] [6] and analog-network coding (ANC) [7] [8]. In both cases, the relay receives the mixed signal, but the difference is that in PNC the relay uses DF strategy, while in ANC the relay employs AF strategy. In this thesis, we choose to use PNC.

To show the throughput advantage of NC in wireless networks, we use the model of a two-way relay channel (TWRC) [9] visualized in Fig. 1.1 [10]. There are two terminals A and B intending to exchange packets a and b, and the link between them is through a relay station R. In the conventional non-NC scheme as in Fig. 1.1(a), terminal A and terminal B each needs one time-slot (TS) to send a packet to the relay, and the relay requires two TSs to broadcast two packets. Hence, the exchange of two packets between two terminals in this case requires four TSs. Fig. 1.1(b) shows that this exchange of data can be accomplished in three TSs: after terminals send their packets independently to the relay in two TSs, the relay employs NC technique to combine (XOR in bit level) the received two packets and broadcasts it in the third TS. The terminals receive the same combined packet but each of them can decode the packet with the knowledge of its own transmitted one. When employing PNC or

ANC, the process only requires two TSs as illustrated in Fig. 1.1(c). Terminals A and B simultaneously transmit their packets to the relay with in-the-air addition of packets, and the relay re-broadcasts the mixed (or XORed representation of) packet it receives.

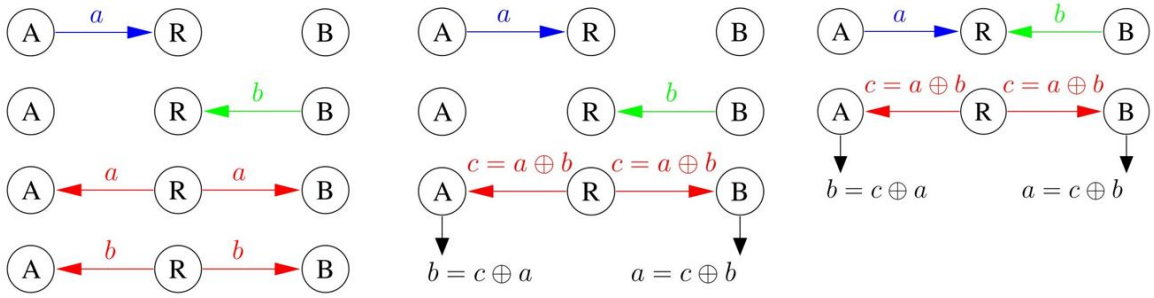

Figure 1.1: (a) Traditional non-NC vs. (b) Traditional NC vs. (c) PNC.

1.2 Signal Alignment

Although the broadcast nature of the wireless channel boosts the capability of NC to improve network throughput, it also brings interference when multiple users transmit signals in the same frequency band at the same time without orthogonal multiplexing. Many investigations have been made and many approaches have been developed to handle this interference. Recently, the IA proposed by Jafar *et al.* [11]–[13] has drawn increasing attention to combat the MAI problem. IA is a cooperative interference management strategy that attempts to align interfering signals in time, frequency, or space. Its basic concept is to overlap interference signals to a small signaling subspace at the receiver via linear precoding vectors at users and to let the desired signals utilize most of the channel resources.

IA provides insight into the signal dimension spatial management and has led to the research of feasibility of SA [14] [15]. In SA, every signal is meaningful for some terminals so that all signal dimension subspace is available for desired signals, which results in higher efficiency than IA. SA focuses on aligning signals with mutual interests to the same dimension for combining them as a whole to proceed with detection and encoding at the relay. For example, Fig. 1.2 shows a six-user TWRC

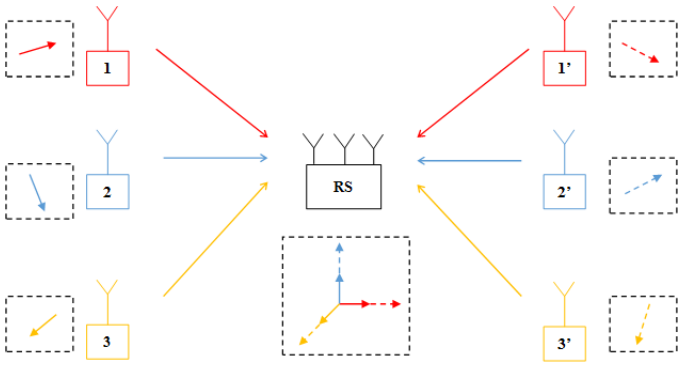

Figure 1.2: 3-paired TWRC with SA.

model where the terminals, indexed by j and j' ($j, j' \in \{1, 2, 3\}$) and each equipped with one antenna, are paired into three groups denoted by different colors. Between each pair, two packets intend to be exchanged via the relay station equipped with three antennas. Precoding vectors, also called beamforming vectors, are carefully selected by paired users so that the precoding vectors combined with the channel matrix can align the signals from paired users into one spatial dimension. Hence, the six messages sent by the six terminals are aligned in three spatial dimensions denoted by colors and combined as three aligned signals which are received at the relay. Then the relay decodes and re-encodes the received signals, so that different colored signals are in different dimensions after being broadcast by the relay. Finally, each terminal can receive signals on the selected dimensions that carry the desired signal and decode the desired information. As this example shows, SA provides superior bandwidth efficiency by exchanging six messages within two TSs. Moreover, because the six signals are aligned into three signals in the air, three antennas are required at the relay, compared with using the MIMO system without NC, where six antennas are needed for receiving six signals.

1.3 MIMO Y Channel Model

The MIMO Y channel proposed by Lee [14] is a generalized model of a wireless TWRC with three users. In this system, the users and the relay are equipped with N_u and N_r antennas respectively, and the antenna configuration must satisfy the condition $2N_u - N_r \geq 1$ to meet the SA requirements. Fig. 1.3 illustrates the minimum antenna configuration MIMO Y channel with three user nodes indexed by i ($i \in$

$\{1, 2, 3\}$) equipped with two antennas and one relay station equipped with three antennas. Each user i has two messages for the other users, denoted as $b_{j,i}$ ($j \in \{1, 2, 3\},\ j \neq i$) and $b_{j,i} \in \{1, 0\}$ at the bit level. If BPSK modulation is applied, the symbol representation of $b_{j,i}$ is $s_{j,i} \in \{1, -1\}$. The traditional assumptions for MIMO Y channel is that all nodes work in half duplex mode and the perfect global channel state information (CSI) is available at all nodes. When users transmit messages to the relay, it is called the MAC phase; and when the relay broadcasts signals to users, it is called the BC phase. The six messages are exchanged within two TSs in MIMO Y channels.

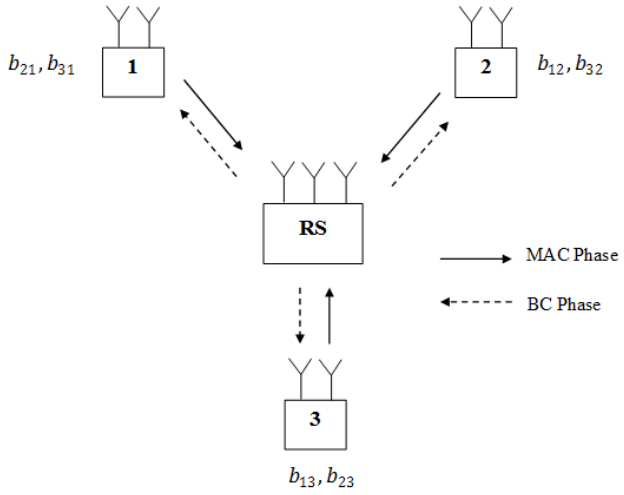

Figure 1.3: The original 3-user MIMO Y channel model.

1.3.1 MAC Phase

In the MAC phase, each user selects two precoding vectors for processing their two transmit messages, and then all users convey a total of six processed messages to the relay simultaneously. Precoding vectors and the channel matrices will align the two mutual signals to a dimension in the signal space, so that the received signal at the relay is actually a superposed signal of three aligned signals in different dimensions. Then the relay decodes three aligned signals with DF strategies.

Fig. 1.4 demonstrates the obtained aligned dimensions through SA which are denoted by D_{12}, D_{13} and D_{23}, and the subscripts represent that this aligned dimension is for mutual symbols between the corresponding users. For instance, D_{12} is the

aligned dimension for mutual symbols $s_{2,1}$ and $s_{1,2}$. The aligned dimensions are determined by the product of the channel gain matrix $H_{r,i}$ and the precoding vector $v_{j,i}$. $H_{r,i}$ is a 3×2 matrix with each entry of $H_{r,i}(t, f)$ indicating the gain from transmit antenna f of the i-th terminal to the receive antenna t of the relay R. The colors in Fig. 1.4 represent different users.

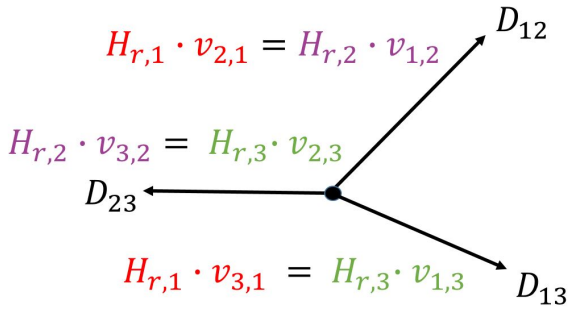

Figure 1.4: The three aligned dimensions for mutual symbols using SA in a 3-user MIMO Y channel in the MAC phase.

Two information symbols $s_{l,i}$ and $s_{p,i}$ $(l, p = \{1, 2, 3\}; l, p \neq i)$ are pre-processed by the precoding matrix $v_i = [v_{l,i} \mid v_{p,i}]$ of size 2×2 at user i where the precoding vectors $v_{l,i}$ and $v_{p,i}$ are of size 2×1. Then the transmitted data by terminal i is $v_i \cdot \begin{bmatrix} s_{l,i} \\ s_{p,i} \end{bmatrix}$ and the received signal from user i at the relay is $H_{r,i} \cdot v_i \cdot \begin{bmatrix} s_{l,k} \\ s_{p,k} \end{bmatrix}$.

The common power assumptions for the MIMO Y channel model are that (i) the average power of information symbols is one and (ii) the total transmit power in the system is constrained to one. The average transmit power P_i for one user can be calculated as:

$$\begin{aligned} P_i &= E\left\{(v_{l,i} \cdot s_{l,i})^H \cdot (v_{l,i} \cdot s_{l,i}) + (v_{p,i} \cdot s_{p,i})^H \cdot v_{p,i} \cdot s_{p,i})\right\} \\ &= E\left\{v_{l,i}^H \cdot v_{l,i} + v_{p,i}^H \cdot v_{p,i}\right\} \end{aligned} \tag{1.1}$$

where $E\{x\}$ is the expectation of random variable x. As indicated in (1.1), when the average power of information symbols is constrained to one, the transmit power is only defined by the square of norms of precoding vectors. In addition, we assume the sum power for transmitting a pair of mutual symbols are the same, so the transmit

power for the whole system P_T can be calculated as:

$$\begin{aligned} P_T &= \sum_{i=1}^{3} \left\{ v_{l,i}^H \cdot v_{l,i} + v_{p,i}^H \cdot v_{p,i} \right\} \\ &= |v_{2,1}|^2 + |v_{3,1}|^2 + |v_{1,2}|^2 + |v_{3,2}|^2 + |v_{1,3}|^2 + |v_{2,3}|^2 \\ &= (|v_{2,1}|^2 + |v_{1,2}|^2) + (|v_{3,1}|^2 + |v_{1,3}|^2) + (|v_{3,2}|^2 + |v_{2,3}|^2) = \frac{1}{3} + \frac{1}{3} + \frac{1}{3} = 1 \end{aligned} \tag{1.2}$$

where $|x|$ is the norm of the vector x.

To control the signaling dimensions used for decoding at the relay, we can only change the precoding vectors, as the channel matrix is determined by the system environment. The precoding vectors are designed and selected in such a way that the product of the channel gain matrix and the precoding vector of the mutual signals are the same as shown in Fig. 1.4. Hence the requirements for the precoding vectors to implement SA are shown below:

$$\begin{cases} D_{12} = H_{r,1} \cdot v_{2,1} = H_{r,2} \cdot v_{1,2} \\ D_{13} = H_{r,1} \cdot v_{3,1} = H_{r,3} \cdot v_{1,3} \\ D_{23} = H_{r,2} \cdot v_{3,2} = H_{r,3} \cdot v_{2,3} \end{cases} \tag{1.3}$$

After the SA requirements are met by processing messages with proper precoding vectors, the signal received at the relay is:

$$\begin{aligned} y_r &= (H_{r,1} \cdot v_{2,1} \cdot s_{2,1} + H_{r,2} \cdot v_{1,2} \cdot s_{1,2}) \\ &\quad + (H_{r,1} \cdot v_{3,1} \cdot s_{3,1} + H_{r,3} \cdot v_{1,3} \cdot s_{1,3}) \\ &\quad + (H_{r,2} \cdot v_{3,2} \cdot s_{3,2} + H_{r,3} \cdot v_{2,3} \cdot s_{2,3}) + n_r \\ &= D_{12} \cdot s_{12} + D_{13} \cdot s_{13} + D_{23} \cdot s_{23} + n_r \\ &= D \cdot [s_{12}, s_{13}, s_{23}]^H + n_r \end{aligned} \tag{1.4}$$

where D is of size 3×3 and is the concatenation of D_{12}, D_{13} and D_{23}, and $s_{ij} = s_{i,j} + s_{j,i}$. It is worth observing that if $s_{i,j} = \pm 1$ then $s_{ij} = \pm 2$ or 0.

At this point, the relay can use the zero-forcing (ZF) approach by multiplying the received signal with the inverse matrix of D [16]–[18], or minimum mean square error (MMSE) [19] or maximum likelihood (ML) decoder to recover each aligned signal [20]. When BPSK is the modulation scheme for users, the decoded signals are ternary symbols at the relay. To simplify decoding for users, the relay encodes the

decoded symbols. Specifically, ± 2 is encoded as 0, and 0 is encoded as 1 [5], so that the bits that the relay broadcasts are $(b_{2,1} \oplus b_{1,2}), (b_{3,1} \oplus b_{1,3}), (b_{2,3} \oplus b_{3,2})$, and users can easily use XOR operation to obtain the desired messages.

1.3.2 BC Phase

In the BC phase, the relay broadcasts aligned signals to users, and users only decode signals from the dimensions that carry the desired signals. To allow users to have the ability to recover signals of interest, a pre-processing of signals with precoding vectors at the relay must be deployed. There are two methods to obtain the precoding vectors in the BC phase. One way is to use nulling precoding vectors that exploit the effects of the channel matrix between the relay and the user, so that destination terminals will not receive the signal processed by this nulling vector [14]. Another approach is based on the reciprocity assumption that $H_{r,i} = H_{i,r}^H$.

In the first method, the nulling vectors for each aligned symbol are denoted by U_{12}, U_{13} and U_{23}, each of size 3×1. The signal transmitted from the relay x_r of size 3×1 can be represented as:

$$\begin{aligned} x_r &= U_{12} \cdot s_{12} + U_{13} \cdot s_{13} + U_{23} \cdot s_{23} \\ &= U \cdot [s_{12}, s_{13}, s_{23}]^H \end{aligned} \tag{1.5}$$

where U of size 3×3 is the concatenation of U_{12}, U_{13} and U_{23}. To prevent users receiving undesired aligned signals (e.g., user 1 is not interested in the aligned symbol s_{23}), the nulling vectors need to satisfy the following equations:

$$\begin{cases} H_{1,r} \cdot U_{23} = 0 \\ H_{2,r} \cdot U_{13} = 0 \\ H_{3,r} \cdot U_{12} = 0 \end{cases} \tag{1.6}$$

Each equation in (1.6) is equal to three unknowns and three linear equations, so there is a solution for each nulling vector. Then we take user 1 for instance and it will receive:

$$\begin{aligned} y_{1,r} &= H_{1,r} \cdot U \cdot [s_{12}, s_{13}, s_{23}]^H \\ &= H_{1,r} \cdot U_{12} \cdot s_{12} + H_{1,r} \cdot U_{13} \cdot s_{13} + H_{1,r} \cdot U_{23} \cdot s_{23} \\ &= H_{1,r} \cdot [U_{12} \cdot s_{12} + U_{13} \cdot s_{12}] \end{aligned} \tag{1.7}$$

In the same way, user 2 and user 3 independently receive:

$$y_{2,r} = H_{2,r} \cdot [U_{12} \cdot s_{12} + U_{23} \cdot s_{23}] \tag{1.8}$$

$$y_{3,r} = H_{3,r} \cdot [U_{13} \cdot s_{13} + U_{23} \cdot s_{23}] \tag{1.9}$$

To show how users obtain the desired information bits, we take user 1 as an example. After processing through the channel between the relay and user, the received signal at user 1 is:

$$y_{1,r} = H_{1,r} \cdot U_1 \cdot [s_{12}, s_{13}]^H \tag{1.10}$$

where U_1 is the concatenation of $[U_{12} \mid U_{13}]$. Then user i can decode aligned symbols using matrix U_1 inversion and obtain the desired message from other users by XORing its known bits with the decoded bits:

$$b_{i,j} = b_{j,i} \oplus \left(b_{i,j} \oplus b_{j,i}\right) \tag{1.11}$$

1.4 Bit Loading Algorithm

In this section, we review, in the context of multicarrier transmissions, the concepts of adaptive modulation schemes with modulation level selection and power allocation. The reason for this is that in this thesis we deploy these concepts in the spatial domain of signalling dimensions which constitute parallel channels in the same way that frequency subcarriers do in multicarrier systems.

At the receiver, because of frequency selective channel characteristics, the instantaneous SNR can vary for different subcarriers. Assuming fixed modulation levels and power across all subcarriers, the high instantaneous SNR at the specific subcarrier would result in very low BER, and the subcarrier's low instantaneous SNR would result in high BER. In practical system, usually there is a targeted BER, independent of subcarrier indices. Moreover, transmitting with a fixed power and modulation level requires the overprovisioning of power, and this results in inefficient use of modulation level (bandwidth) on some subcarriers. Hence to obtain the acceptable BER on all subcarriers, the amount of energy and the number of bits allocated to each subchannel should be optimized according to the parallel channel gains (SNRs).

Bit loading algorithms allocate transmit power to each subcarrier based on their channel conditions and then distribute bits to subcarriers to achieve throughput

improvement. There are two major types of bit loading algorithms: (i) minimizes power subject to a data rate and BER constraints, which is called Margin-Adaptive (MA) [21]–[23] and (ii) maximizes spectral efficiency with power and BER constraints, which is called Rate-Adaptive (RA) [24]–[26]. Although the two types have different constraints and objectives, they share the same principle of power efficiency.

In this thesis, in Chapter 4, we attempt to maximize the data rate and in the following sections we present two known algorithms in the literature to reach the maximum throughput with the constraint of fixed total power. First, we describe the water-filling algorithm which is the optimal power allocation strategy that achieves the capacity of parallel channels. Then we explain the operation of a practically implementable algorithm to maximize throughput with a discrete alphabet signalling.

1.4.1 Water-filling Algorithm

As defined in information theory by Shannon, channel capacity is the tight upper bound of the maximum data rate that a channel can reliably transmit without constraints on delay or coding techniques [27]. When the transmitter and the receiver know CSI through channel estimation and transmitter feedback, the optimum power distribution strategy among subchannels to achieve the channel capacity is water-filling.

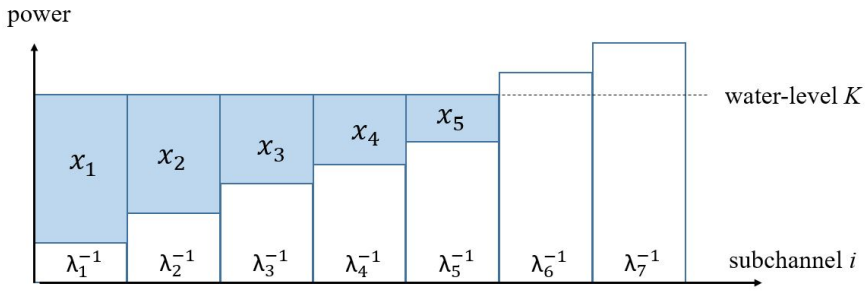

Figure 1.5: Power allocation in the water-filling algorithm.

Fig. 1.5 illustrates the idea of the water-filling algorithm by an example of a system with $N = 7$ subchannels. In the figure, $\sqrt{\lambda_i}$ $(i = (1, 2, ..., 7))$ is the channel gain of the subchannel i and x_i is the power allocated to the subchannel i (the shadow parts). Here, we assume the same noise power for all subcarriers. As presented in the figure, power is distributed to the subchannels like pouring water over a surface.

The allocation of power is based on the inverse of the channel power gain (λ_i), which guarantees that the subchannels with better conditions have more power compared to other subchannels, but as the total amount of power is limited, sometimes the worst subchannels do not have any power and are not used for transmitting [28]–[30].

The water-filling algorithm is to recursively solve $N+1$ unknowns (x_i and K) with $N+1$ equations as given by:

$$\begin{cases} \lambda_i^{-1} + x_i = K \ (i = (1, 2, ..., N)) \\ \sum_{i=1}^{N} x_i = P \end{cases} \tag{1.12}$$

until gaining an acceptable solution. We can obtain one set of solutions from (1.12), but when the solutions include a negative x_i, it indicates that at least one subchannel is not acceptable and should not be used. If the negative power result occurs, we set the lowest x_i in (1.12) to zero and omit the equation with λ_i^{-1}, and then recalculate the equation set. The process is conducted iteratively until all outcomes are non-negative, and then bits are allocated according to the channel conditions and allocated power.

However, the solutions of the water-filling algorithm are of theoretical value to achieve capacity, and the allocated bits per symbol can be any real numbers, which is impractical to implement in the modulation schemes alone [31]. Usually, the discrete modulation schemes such as QAMs and phase shift keying (PSK) are used in adaptive modulations, and for these discrete input alphabets, alternative bit loading algorithms are considered [32].

1.4.2 Discrete Bit Loading Algorithm

Many researchers have investigated the discrete bit loading algorithms, and there are three approaches seen as classic solutions: (i) the Hughes-Hartog algorithm which is based on greedy optimization method [33]; (ii) Chow's algorithm that distributes bits by approximately rounding the water-filling results [34] and (iii) the Fischer-Huber algorithm which provides solutions for systems with the constraints of total energy and data rates [21]. As we aim for throughput improvement, the Fischer-Huber algorithm of the MA type is not suitable; Chow's algorithm is simpler than the Hughes-Hartog algorithm, but it gives the worst performance out of the three methods [35]. Hence, we select the Hughes-Hartog algorithm that offers the optimal

discrete bit loading results.

The Hughes-Hartog algorithm iteratively assigns one bit at a time to the subcarrier that requires the minimum incremental amount of power to transmit one additional bit at a targeted BER until the total power constraint is reached. Specifically, the bit and power allocation proceeds in the following steps: (1) the power needed for transmitting one more bit at a target BER is calculated for each subcarrier based on their subchannel conditions; (2) check if the unallocated power is greater than the minimum power obtained in the previous step; (3) if it is, one bit is assigned to the subcarrier with the minimum required power and the leftover power decreases by the amount of the power needed for this additional bit in this time, then repeat from step (1); if it is not, it means that the leftover power cannot afford to transmit one more bit, and the leftover power is distributed evenly to all subcarriers to enhance their performances, and then power and bit allocations are finished. It should be noted that the increment is one bit for the modulation schemes applied in the Hughes-Hartog algorithm as it assigns power based on comparing the situations of one additional bit transmission for subcarriers.

1.5 Thesis Objectives

This thesis designs a signal alignment scheme that exploits orthogonality of spatial signalling dimensions in the MIMO Y channel to overcome limitations on controlling the minimum distance between signaling points representing network coded messages. This is accomplished by adding one redundant antenna at every user and calculating the corresponding precoding vectors to obtain the flexibility in the selection of orthogonal signaling dimensions as well as to simplify the decoding at the relay. We initially work with BPSK signaling and then we introduce procedures to accommodate higher modulation levels offering the advantage of higher bandwidth utilization. Once we have a baseline for working with different modulation levels, more advanced power allocation and bit loading are proposed to increase the data throughput in the MIMO Y channel.

In the first part, the thesis explores the situation where the signal dimensions of MIMO Y channels are designed to be orthogonal. It brings two advantages: (1) easy decoding process at the relay without noise enhancement present when conventional

zero-forcing decoding algorithms are deployed and (2) improved BER performance for user pairs though these improvements are unbalanced for different user pairs. For BPSK signaling, we even the performances via power allocation to distribute energy among the users based on their channel conditions. In addition, iterative optimization of the signaling dimensions and time scheduling of transmissions according to channel states are employed to further improve the BER performance.

In the second part, this thesis investigates the deployment of higher level modulations at users sides and the corresponding decoding at the relay with a unique bit mapping strategy. Bit loading and power allocation strategies are developed to further increase the MIMO Y channel throughput.

The original MIMO Y channel deploys the SA technique which combines two mutual symbols in one dimension in the signaling space. This leads to significant improvement in throughput, but the BER performance is not very good. This is because sometimes the calculated signalling (spatial) dimensions for aligned symbols result in the very low minimum distance between the symbols, and this affects symbol error rate (SER) performance. The motivation for our work was that by ensuring orthogonality of spatial dimensions, we will not only simplify the decoding process but we will also control better the minimum distance between the signaling points and thus reduce SER. Therefore, we attempt to add flexibility in the selection of signaling dimensions to be able to work with orthogonal dimensions. By adding redundant antennas and using iterative search, the signaling dimensions with best effective channel gain for the aligned symbols are selected. In fact, the more redundant antennas are used, the more diversity gain is introduced; and the more iterations are applied, the more opportunity there is to obtain the better signaling dimension for better BER performance. However, in reality, applications require simplicity and efficiency, and adding many redundant antennas and exhaustive searches for better signaling dimensions fail these requirements. These are the reasons why sometimes in our work we were pursuing suboptimum solutions using algorithms with lower computational complexity.

One of the main contribution in this thesis is the constellation mapping of QAM symbols in the MIMO Y channel. As presented in the thesis, the constellation of received aligned symbols at the relay is much more complex than the symbols sent

from users. To reduce the decoding calculations for all users, the relay can conduct decoding for users and then re-encode the symbols to a smaller (original) constellation.

The generic ML decoding implemented through minimum distance decoding is the optimal method which minimizes the symbol error rate, but its application is computationally intensive in the MIMO Y channel at the relay. On the other hand, ZF decoding is much easier but it suffers from noise enhancement, which sometimes has negative effects on BER. The proposed scheme with only one extra antenna at each user side builds on the fact that this antenna configuration offers infinite possible combinations of the signal dimension selections. To efficiently decide the aligned signal dimensions, we introduce the orthogonality constraint to the selection of the dimensions. The proposed scheme with orthogonal signaling provides a simple way to perform the decoding in MIMO Y channels through slicing of coordinates along the orthogonal dimensions and is equivalent to ML decoding with hyper-cube signaling as shown in Fig. 1.6. In hyper-cube signaling, a received signal is in a 3-dimensional (3D) space that can be represented by three orthogonal coordinate axes, and this signal can be decoded into three bits. Each bit is decided by the projection of the signal on one axis: according to the distance of the projected coordinate and two possible points on that dimension, the closest point is chosen to be the transmitted symbol and one bit is decoded based on the selected symbol. The difference is that in hyper-cube signaling, each dimension has two levels, while in the proposed scheme, each signaling dimension has multiple levels that are determined by superposed symbols and their modulation type used at users.

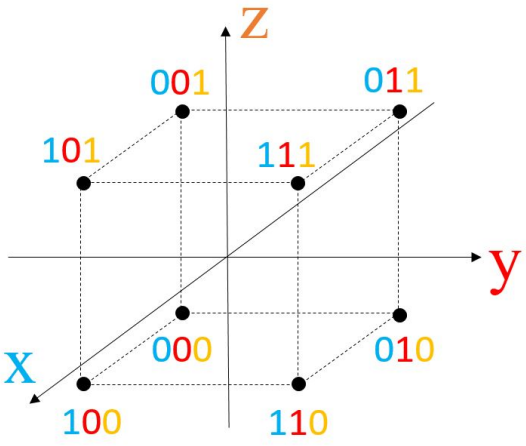

Figure 1.6: The Hyper-cube signaling.

1.6 Thesis Organization

The remainder of this thesis is organized as follows:

In Chapter 2, we propose the design of orthogonal signal dimensions for MIMO Y channels which simplifies the ML decoding process. Computationally efficient method is developed to calculate the precoding vectors; however, the method introduces unbalanced BER performance among different users. To alleviate the problem and further improve BER performance, different modifications in the original orthogonal signal alignment scheme are proposed. As demonstrated through simulations, all proposed schemes with BPSK signaling show improvement in the BER performance over the original MIMO Y channel scheme.

In Chapter 3, we first present the QAM constellation mapping in the MIMO Y channel to improve the system throughput. This is done through the bit mapping at the user side and the extended constellation decoding at the relay. Then we develop the bit loading algorithm to improve the utilization of bandwidth and power in the system. The modulation selected in bit loading for each user pair depends on the instantaneous SNR of the aligned symbol links. Hence, when power allocation is done using bit loading, it maximizes the system throughput.

Chapter 4 presents the contributions of this thesis and the potential for future investigations.

Appendix A derives the BER performance of the superposed constellations at the relay which is used in Chapter 3.

Chapter 2

Orthogonal Signal Space Alignment for MIMO Y Channels

The antenna configuration in the original MIMO Y channel system imposes limitations on controlling the minimum distance between signaling points representing network coded messages, which affects BER performance. To mitigate this problem, we add one redundant antenna at every user and design the corresponding precoding vectors to obtain flexibility in the selection of orthogonal signaling dimensions and to simplify decoding at the relay. The design of precoding vectors in the proposed scheme improves the total BER performance despite the BER is not balanced among the three users. To even the performance, the power allocation and iterative search can be applied to distribute energy among the users based on their channel conditions. In addition, the optimization of the signaling dimension orientation and time scheduling are deployed to further improve the BER performance.

This chapter is organized as follows. First, Section 2.1 presents the previous work focused on improving BER performance for MIMO Y channels. Section 2.2 demonstrates the proposed system model. Next, Section 2.3 describes the advantages of applying orthogonality, and the constraints for introducing orthogonality into MIMO Y channel, as well as a simple method to conducting the calculations of precoding vectors. Section 2.4 presents further modifications for the proposed scheme which lead to better BER performance. Finally, different results are summarized and compared in Section 2.5.

2.1 Related Literature Evaluation

In order to accommodate the two mutual messages into one dimension in the signal space, multiple antennas are required. However, with the minimum antenna configuration ($N_u = 2$ and $N_r = 3$), the BER performance of MIMO Y channel is not ideal even with large transmit SNR, because sometimes the spatial dimensions formed by the precoding vectors and channel matrices do not make the best use of the

aligned signal power. Moreover, the precoding vectors generated from the minimum configuration are unique and we cannot avoid the situations when the undesired spatial dimensions appear. Hence, some designs have been studied applying more antennas to obtain more degrees of freedom for improving BER performance.

In [16], using redundant antennas, $2N_u - N_r$ random iterations are used to generate different beamforming vectors, and the set of precoding vectors that can provide the best BER performance is selected as the final ones for the system. This algorithm shows improvement compared to the minimum antenna configuration scheme, but the random selection in the signal space may miss the opportunities for better performance. Another iterative beamforming optimization algorithm is proposed in [18] based on orthogonal projections in the signaling space, which shows much improvement in the BER performance. However, the beamforming vectors in this design are formed and selected through very complex calculations, and because of the irregularity that appeared in iterations, it is difficult to theoretically proof the convergence. An algorithm with lower computational complexity called an iterative interference alignment is presented in [19], where in MAC phase precoding vectors and combining vectors which are used for decoding at the relay are iteratively optimized at transmitters and receivers. This aims to minimize the effects of interference signals from the desired signals. However, in this algorithm, in each iteration the precoding vectors and combining vectors are both considered, and the number of iterations required for convergence is large. Moreover, [36] proposes antenna selection among redundant antennas at users and the relay, but it is not ideal for practical applications because the level of BER improvement depends on the number of used redundant antennas.

2.2 System Model

We use the MIMO Y channel model as in Fig. 2.1 where each user and the relay have three antennas. In our derivation of orthogonal signaling in this case, we follow in this chapter the notations introduced in Section 1.3. The only difference between the proposed system model and the original one is the number of antennas at users, which will change the channel matrices' size to 3×3 and the precoding vectors' size to 3×1.

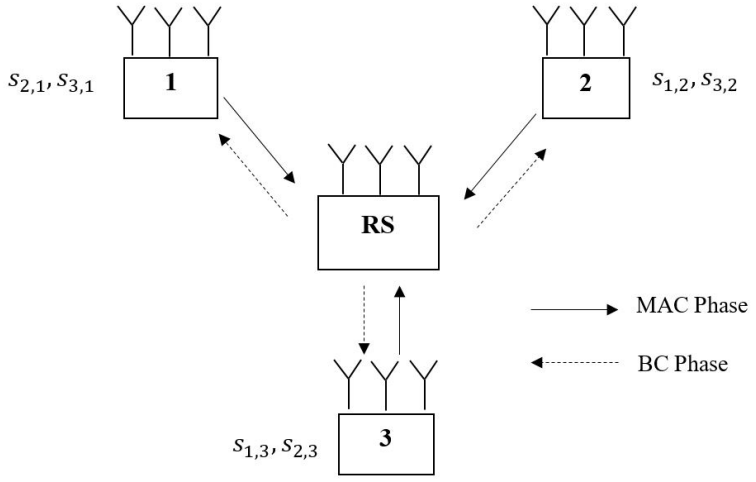

Figure 2.1: The proposed 3-user MIMO Y channel model.

In the original MIMO Y channel, each user is equipped with two antennas, resulting in $H_{r,i}$ being of size 3×2 and each precoding vector of size 2×1. For each constraint in (1.3), there are four unknowns representing entries in two precoding vectors and three linear equations, which implies a unique solution to the direction of one pair of precoding vectors except for a parameter of scaling. Hence, the three signaling dimensions determined in the original MIMO Y channel are fixed. After the dimensions are obtained, we also need to impose the limits on the power of the precoding vectors ($|v_{j,i}|^2 = v_{j,i}^H \cdot v_{j,i}$) to meet the power constraint in (1.2). This power limit adds a constraint to the scaling parameters of precoding vectors, which will partially influence the effective channel gain. However, because of the Rayleigh fading channels, the effective gains $|D_{12}|$, $|D_{13}|$ and $|D_{23}|$ are different and varying, the distance between the closest aligned symbols in 3D signaling space at the relay may be large for separating some aligned symbols and small for others. The average BER performance is eventually determined by the minimum distance between the aligned symbols which cannot be controlled in the original MIMO Y channel scheme.

The problem is visualized in Fig. 2.2, when the relay receives signals with the ternary symbol coordinates for the case where the terminals are using BPSK. Actually, there are $3^3 = 27$ possible superposed symbols of the three aligned symbols received at the relay as illustrated in Fig. 2.3. But in Fig. 2.2 we only show their coordinates in the similar way as in quadrature phase shift keying (QPSK), where quaternary symbols can be scrutinized through the coordinates of BPSK along the in-phase

and the quadrature components (corresponding to D_{12}, D_{13} and D_{23}). The major difference here is that while for QPSK, the in-phase and quadrature directions are orthogonal, in the original MIMO Y channel SA, the directions D_{12}, D_{13} and D_{23} are not. Another difference is that the norms $|D_{12}|$, $|D_{13}|$ and $|D_{23}|$ are normally not equal, and the minimum distances for different signal pairs are random and can be very small occasionally. However, when averaging the BER over the Rayleigh channels, the BER performance is always determined by the minimum distance or the worst scenarios. This means that in a MIMO Y channel, we would have larger minimum distance and effective channel gains if we could utilize directions well.

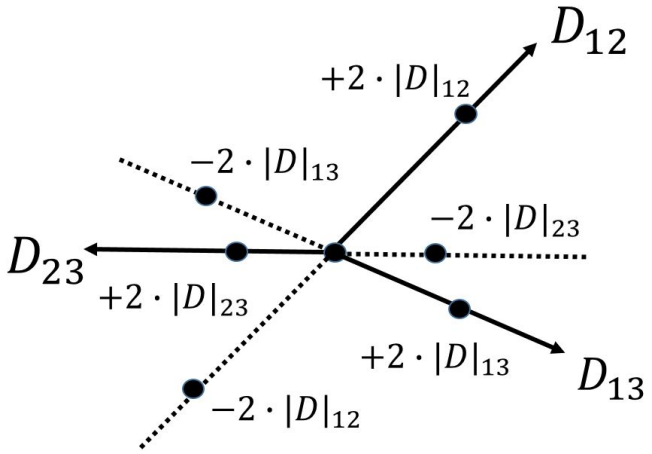

Figure 2.2: Possible coordinates along D_{12}, D_{13} and D_{23} for received symbols at the relay in 3D.

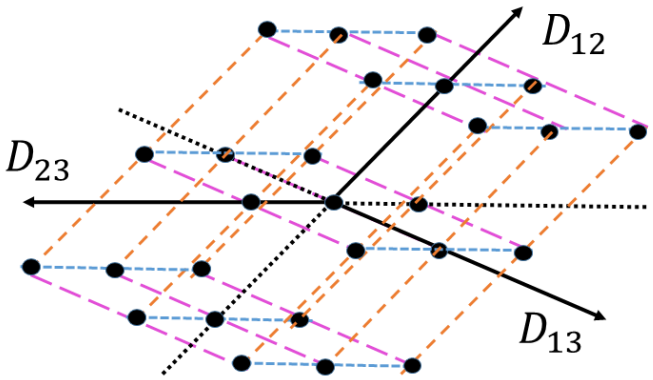

Figure 2.3: The possible signal received at the relay through the signal summation over the air.

In the MIMO Y channel model adopted in this thesis, each terminal and the relay are equipped with three antennas, so that $H_{r,i}$ and precoding vectors $v_{l,i}$ and $v_{p,i}$ are of size 3×3 and 3×1, respectively. There are six unknowns (representing entries in two precoding vectors) and three linear equations for each constraint in (1.3), resulting in the solutions for a pair of precoding vectors being in the 3D space. Therefore, the choices for the aligned dimensions D_{12}, D_{13} and D_{23} (determined by precoding vectors) are much more flexible than in the original MIMO Y channel. We exploit this potential advantage in the following section.

After the relay receives signals, a decoding process is conducted normally by ZF, MMSE or ML methods to obtain the aligned symbols, and the decoded aligned symbols are remapped to BPSK again for simple decoding for users. Next, a new set of precoding/nulling vectors are applied to the aligned symbols before sending to users. Each user i will only receive two desired aligned symbols s_{ip} and s_{il} from two of the three dimensions that are generated in the BC phase. Then for each received symbol s_{ij}, user i has the knowledge of its transmitted symbol $s_{j,i}$ and can use XOR operation to obtain the desired message $s_{i,j}$. In this thesis, we focus on the MAC phase because, as demonstrated in [16], the precoding vectors from MAC phase can also be calculated to obtain the precoding vectors in the BC phase. On the other hand, we can also apply the antenna selection to benefit from receiver selection diversity in the BC phase. In this way, two out of three antennas are chosen at each user based on channel conditions to form the minimum configuration of MIMO Y channels and the nulling vectors are used at the relay.

2.3 Orthogonality Application

2.3.1 ML Receiver

In most publications on the MIMO Y channel, the relay obtains the network-coded version of paired messages by using the ZF, MMSE or ML decoders. In the MAC phase, we decide on the three ternary aligned symbols s_{12}, s_{13} and s_{23} of levels $\pm 2,\ 0$. In this case, the ML decoding is equivalent to the minimum distance decoding of $3^3 = 27$ ideal symbols visualized in Fig. 2.3. These points are located in 3D space with positions determined by coordinates $(\pm 2,\ 0) \cdot |D_{12}|$, $(\pm 2,\ 0) \cdot |D_{13}|$ and $(\pm 2,\ 0) \cdot |D_{23}|$. Obtaining the received signal coordinates and using Voronoi regions

for ML decoding do not work in the original MIMO Y channel because the decision rules are very complex and one needs to evaluate 27 Euclidean distances in 3D for each packet. In the ZF approach, the recovery of the signal of interest is obtained rather simply by inverting the matrix $[D_{12}|D_{13}|D_{23}]$ and multiplying the received vector, but this method suffers from noise enhancement. In general, when compared to ZF decoding, ML gives better performance (13dB gain at the BER of 10^{-3}) but requires higher computational complexity [20]. This motivates the investigation in this thesis where we attempt to work with a simpler implementation of the ML receiver by sacrificing some performance loss (in terms of BER) as a result of using a constellation of points similar to hyper-cube signaling and a higher number of antennas. Specifically, by imposing the orthogonality requirements, we simplify the ML decoding at the relay to just projecting the received signal and slicing them along three orthogonal directions D_{12}, D_{13} and D_{23}. In 2D, this corresponds to interpreting quadrature amplitude modulation (QAM) or QPSK decoding as pulse amplitude modulation (PAM) decoding along the orthogonal in-phase and quadrature directions. In 3D, this approach is equivalent to decoding the hyper-cube signal as in Fig. 1.6.

2.3.2 Orthogonality Constraints

As presented in the previous section, in the underlying system model, the SA requirement for each signaling dimension constraint in (1.3) results in the solutions to a pair of precoding vectors being in a 3D space. Because any pair of precoding vectors in a 3D space defined by (1.3) can satisfy the SA requirement, we will utilize this freedom by imposing extra conditions on precoding vectors (or equivalently signaling dimensions). This is with the purpose to select precoding vectors that offer benefits in terms of improved BER compared to ZF and to simplify the decoding process compared to ML. Specifically, the proposed orthogonal signal alignment scheme constrains the signaling dimensions to satisfy the following orthogonality conditions:

$$\begin{cases} D_{12}^H \cdot D_{13} = 0 \\ D_{12}^H \cdot D_{23} = 0 \\ D_{13}^H \cdot D_{23} = 0 \end{cases} \tag{2.1}$$

where $\{\cdot\}^H$ means Hermitian transpose. These are the additional constraints on precoding vectors on top of those in (1.3).

2.3.3 Calculations of Precoding Vectors

We assume that the total transmit power $P_T = 1$ is as in (1.2). To meet this standard condition in the system under study, we work with the additional assumption that the power for user i and user j to transmit their mutual symbols $s_{i,j}$ and $s_{j,i}$ that become an aligned symbol is constrained to $\frac{1}{3}$, i.e., $v_{i,j}^H \cdot v_{i,j} + v_{j,i}^H \cdot v_{j,i} = \frac{1}{3}$ [20]. In this way, we will analyze from the perspective of the links between users for simplicity rather than users as each user accounts for two links which would be more complex to discuss results.

Our objective is to calculate the precoding vectors (for each information symbol) that will satisfy (i) the SA conditions in (1.3); (ii) signaling dimensions orthogonality in (2.1) and (iii) the power limit (1.2). There is a total of six precoding vectors, and each precoding vector is a matrix of 3×1, hence there are 18 scalar unknown values. The nine linear equations in (1.3) and the three quadratic equations from (2.1) compose a system of equations that will still give ample opportunities for choosing precoding vectors. To reduce the complexity of solving these equations, we handle the equation sets in a specialized sequence of steps involving linear matrix operations presented next.

Before proceeding for the proposed SA, we rearrange our mathematical representations into more convenient forms. In particular, we substitute $(H_{r,2} \cdot v_{1,2})$, $(H_{r,3} \cdot v_{1,3})$ and $(H_{r,3} \cdot v_{2,3})$ for D_{12}, D_{13} and D_{23}, respectively, which gives the equivalent requirement to (2.1) as:

$$\begin{cases} (H_{r,2} \cdot v_{1,2})^H \cdot (H_{r,3} \cdot v_{1,3}) = 0 \\ (H_{r,2} \cdot v_{1,2})^H \cdot (H_{r,3} \cdot v_{2,3}) = 0 \\ (H_{r,3} \cdot v_{1,3})^H \cdot (H_{r,3} \cdot v_{2,3}) = 0 \end{cases} \tag{2.2}$$

We also transform the first equation in (1.3) into:

$$\begin{bmatrix} v_{2,1} \\ v_{1,2} \end{bmatrix} = null[H_{r,1} \quad -H_{r,2}] \tag{2.3}$$

where $null[A]$ represents the null space of matrix A. $[H_{r,1} \ -H_{r,2}]$ is a 3×6 matrix

which with high likelihood has a full rank, hence the null space of this matrix has $6-3=3$ dimensions and each dimension is represented by a vector of size 6×1. These three dimensions are the orthogonal basis obtained from the singular value decomposition for the null space of $[H_{r,1}\ -H_{r,2}]$, and the vector $\left[\begin{smallmatrix} v_{2,1} \\ v_{1,2} \end{smallmatrix}\right]$ can be equal to any linear combination of these basis. That is to say, any vector in this null space meets the requirement for $v_{2,1}$ and $v_{1,2}$ to align the mutual symbols. It should be noted that there are three parameters for the three basis, which actually determine the aligned dimension. At this point, we cannot decide which vector in this null space is the best choice because in our proposed algorithm, the first selected aligned dimension D_{12} will have influence on the other precoding vectors for D_{13} and D_{23}. Hence, at present, three random parameters are chosen for these basis and we can obtain a 6×1 matrix that decides the direction of the precoding vectors $v_{2,1}$ and $v_{1,2}$. Then we consider the power limitation by normalizing the basis parameters to let $\left[\begin{smallmatrix} v_{2,1} \\ v_{1,2} \end{smallmatrix}\right]^H \cdot \left[\begin{smallmatrix} v_{2,1} \\ v_{1,2} \end{smallmatrix}\right] = \frac{1}{3}$, meaning that the power sum of $v_{2,1}$ and $v_{1,2}$, or the sum of the transmit power for $s_{2,1}$ and $s_{1,2}$, equals to $\frac{1}{3}$. After $v_{2,1}$ and $v_{1,2}$ are decided, D_{12} is obtained as $D_{12}=H_{r,2}\cdot v_{1,2}$.

Once we determine D_{12} as well as $v_{1,2}$, we can find D_{13} and D_{23} with the first two equations in (2.1). Because we are more interested in precoding vectors defining D_{13} and D_{23}, from the equivalent orthogonality requirements in the first two equations in (2.2) we calculate:

$$\begin{cases} v_{1,3} = null(v_{1,2}^H \cdot H_{r,2}^H \cdot H_{r,3}) \\ v_{2,3} = null(v_{1,2}^H \cdot H_{r,2}^H \cdot H_{r,3}) \end{cases} \tag{2.4}$$

which shows the precoding vectors $v_{1,3}$ and $v_{2,3}$ are in the same null space. For each equation in (2.4), the left side is a vector of size 3×1 meaning 3 unknowns, and the right side is a null space of a 1×3 vector meaning one linear equation, so the null space would have $3-1=2$ dimensions and each dimension is represented by a matrix of 3×1. This indicates the null space is a plane where the precoding vectors $v_{1,3}$ and $v_{2,3}$ would be. When deciding on $v_{1,3}$ and $v_{2,3}$, we also need to meet orthogonality requirement between D_{13} and D_{23} as illustrated in the last equation in (2.2). To this end, we use vectors x and y, each of size 3×1, representing the two basis of this null space and we use parameters a_1 and b_1 for representing $v_{1,3}$ with the basis, and a_2

and b_2 to determine $v_{2,3}$ with the basis, i.e., $v_{1,3} = a_1 \cdot x + b_1 \cdot y$ and $v_{2,3} = a_2 \cdot x + b_2 \cdot y$. Now we substitute these representations of $v_{1,3}$ and $v_{2,3}$ to the last equation in (2.2) and obtain the condition for a_1, b_1, a_2, b_2:

$$\begin{bmatrix} a_1 \\ b_1 \end{bmatrix}^H \cdot [x \;\; y]^H \cdot [H_{r,3}]^H \cdot [H_{r,3}] \cdot [x \;\; y] \cdot \begin{bmatrix} a_2 \\ b_2 \end{bmatrix} = 0 \tag{2.5}$$

So far, we cannot directly decide the best parameters a_1, b_1, a_2 and b_2 defining $v_{1,3}$ and $v_{2,3}$. For ease of calculations, we first choose two random values for a_1 and b_1 for determining the direction of $v_{1,3}$, and then use the second equation in (1.3) to get the null space as:

$$\begin{bmatrix} v_{3,1} \\ v_{1,3} \end{bmatrix} = null[H_{r,1} \quad -H_{r,3}] \tag{2.6}$$

Although the basis for this null space has three dimensions, we can have the three parameters for the basis with the knowledge of the determined direction of $v_{1,3}$ and hence obtain $v_{3,1}$. At last, we normalize the 6×1 vector in this null space to $\frac{1}{3}$ to meet the condition for power. With this, D_{13} is determined.

After a_1 and b_1 are selected, (2.5) leaves two unknown parameters a_2 and b_2 defining $v_{2,3}$ which indicates $v_{2,3}$ is a line in the space, so the direction of the precoding vector $v_{2,3}$ is fixed. Next, we transform the last equation in (1.3) to:

$$\begin{bmatrix} v_{3,2} \\ v_{2,3} \end{bmatrix} = null[H_{r,2} \quad -H_{r,3}] \tag{2.7}$$

Still, the basis for this null space has three dimensions, but knowing the direction of $v_{2,3}$, the parameters for the basis in this null space can be decided and then the direction of $v_{3,2}$ is also obtained. Finally, we normalize the parameters to maintain that $|v_{2,3}|^2 + |v_{3,2}|^2 = \frac{1}{3}$. Till this point, all the precoding vectors and the aligned dimensions D_{12}, D_{13} and D_{23} are determined with the mutual orthogonality property.

2.3.4 Performance

In this section, we present the BER performance simulation results in the MAC phase for our proposed scheme and the original MIMO Y channel scheme for comparison. The performance of the schemes without orthogonality are obtained with ZF decoding as it is a widely used method in other research. The transmit SNR is defined here as P_T/σ^2, where σ^2 represents the variance of the noise. Hence, despite

how many antennas users are equipped with, the total transmit power in each system remains the same for fair BER performance comparisons. All the links are assumed to be quasi-static Rayleigh fading channels. The uncoded BPSK is adopted as the modulation format, so that the network coding in the MIMO Y channel is the bit-wise XOR.

The BER performance of the original and the proposed schemes is shown in Fig. 2.4. For the original scheme, three user pairs present the same performance, however, for the proposed scheme the figure shows different results for the three user pairs. *user* $pair_{23}$ appears to have a very close result to the one in the original MIMO Y channel scheme, while for *user* $pair_{13}$ there is an improvement of 5dB at BER 10^{-3}, and for *user* $pair_{12}$ it is even 18dB better than in the original MIMO Y channel scheme. Although the improvements do not distribute equally for the three user pairs, the outcomes show progress in the proposed scheme.

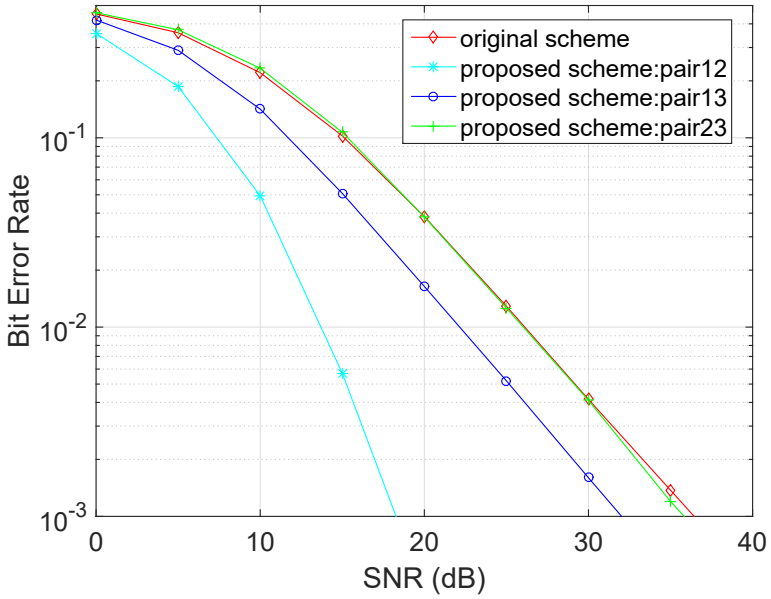

Figure 2.4: The comparison between the BER performances of the original MIMO Y channel scheme and the proposed scheme for different user pairs.

The reasons for unbalanced performance in the proposed scheme are as follows. At the end of the last section, D_{12}, D_{13} and D_{23} are calculated to meet the imposed conditions for SA and orthogonality which may seem symmetrical. However, due to the sequence of steps when solving the equation sets, the average powers of D_{12}, D_{13} and D_{23} show difference: $|D_{12}|^2$ is the largest and then is $|D_{13}|^2$, and $|D_{23}|^2$ is the

minimum; and hence the performance of user pairs on different dimensions appears to be unbalanced. The *user pair*$_{12}$ on D_{12} has the best BER because the precoding vectors for D_{12} is first decided and have a 3D space selection range, while *user pair*$_{23}$ on D_{23} shows the worst BER for the precoding vectors of D_{23} are determined last and only have one direction.

In addition, in Fig. 2.5, we present the throughput of the proposed scheme. Throughput is defined here as the number of correctly received bits per time slot per user pair. As the figure shows, the proposed scheme provides three different throughput curves for the three user pairs, corresponding to their BER performance (better BER performances lead to higher throughputs). In the original MIMO Y channel, the three user pairs would have the same throughput similar to the *user pair*$_{23}$ has in the proposed scheme. When the BER performance is near 10^{-3} for each user pair, the throughput for that pair is very close to one, which is the maximum that the BPSK modulation can supply, and it demonstrates that in this scheme, the BER 10^{-3} would be considered as an acceptable value for the system and will be used in the following parts.

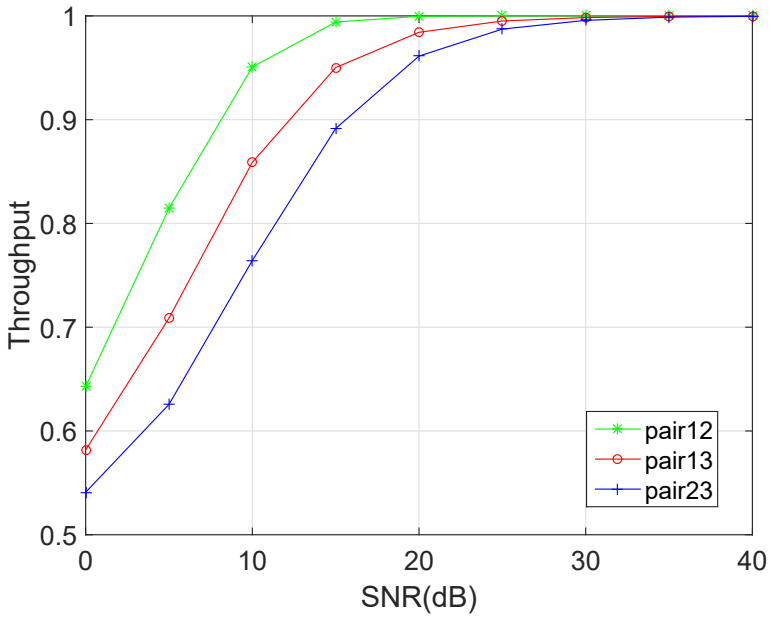

Figure 2.5: The throughput in the proposed scheme for different user pairs.

2.4 Modifications in Orthogonal Signaling

2.4.1 Power Allocation

We observe that the mutual symbols on D_{12} have the most improvement in BER reduction over the conventional MIMO Y channel scheme, and the symbols on D_{23} have the minimal improvement. To let the performance be fair for each user pair, we propose to apply power allocation to adjust the transmit power based on precoding vectors depending on their channel characteristics.

As in Section 2.3.3, the sum power for transmitting mutual symbols is initially fixed to $\frac{1}{3}$, but when the aligned dimensions are obtained through the process in Section 2.3.3, the mean values of the effective channel power gains ($|D_{12}|^2$, $|D_{13}|^2$ and $|D_{23}|^2$) are dissimilar: $E\{|D_{12}|^2\}$ is the largest and $E\{|D_{23}|^2\}$ is the smallest. This is consistent with the BER performance of the three user pairs in Section 2.3.4. To balance the outcomes, we attempt to retain the power equilibrium among the three dimensions by adjusting the transmit power of users. We insert scaling factors to the precoding vectors, and the representation of total transmit power is changed from (1.2) to:

$$p_{12}\cdot(|v_{2,1}|^2+|v_{1,2}|^2)+p_{13}\cdot(|v_{1,3}|^2+|v_{3,1}|^2)+p_{23}\cdot(|v_{2,3}|^2+|v_{3,2}|^2)=1 \tag{2.8}$$

where, because of (1.3), p_{12}, p_{13} and p_{23} are the power scaling parameters for D_{12}, D_{13} and D_{23}, respectively. In order to let all aligned symbols received at the relay have the same norm for the effective channel gains (which for orthogonal signaling means the same minimum distance) without modifying the total power limit, the following relations are established:

$$\begin{cases} p_{12}\cdot|D_{12}|^2 = p_{13}\cdot|D_{13}|^2 \\ p_{12}\cdot|D_{12}|^2 = p_{23}\cdot|D_{23}|^2 \\ p_{12}+p_{13}+p_{23}=3 \end{cases} \tag{2.9}$$

when solving for p_{12}, p_{13} and p_{23} which control improved effective channel gains. In essence, the power scaling parameters p_{12}, p_{13} and p_{23} redistribute the power from the user pairs with better BER to compensate the user pair with the worst BER while maintaining the same total power as in the original system.

The results are demonstrated in Fig. 2.6, where the three user pairs have matching performance. This BER outcome is 4dB better than the original scheme. This is because even though the result here is the average of the proposed three user pair performances in Fig. 2.4 where one user pair's BER performance is considerably better than the one in the original scheme, the whole system is still under the major influence of the worst link. Furthermore, comparing the BER results with the ones in Fig. 2.4, it can be observed that the averaged performance is 4dB better than the worst user pair but it is 15dB worse than the best user pair in the original orthogonal signal alignment. Therefore, it seems inefficient to sacrifice a noteworthy gain from a user pair with good performance to improve a little for another user pair. Again, it is proven that for the BER performance the worst scenario has the most important weighing factor for the total system.

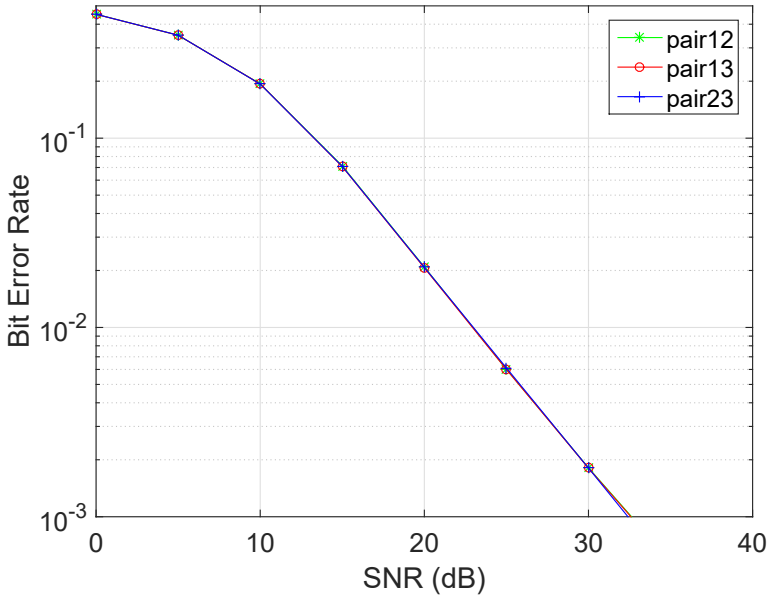

Figure 2.6: The BER performance of the proposed MIMO Y channel scheme with power allocation.

2.4.2 Time Scheduling

Even though the power allocation can equalize the BER performance for the three user pairs, the balanced result is dominated by the worst user pair's performance. Hence we propose to control the occurrences of the worst scenarios by imposing limitations in time on terminals accessing the orthogonal spatial streams when the

channel conditions result in any of the effective channel power gains $|D_{12}|^2$, $|D_{13}|^2$ and $|D_{23}|^2$ below a predefined threshold. If the powers of signalling dimensions fall below a certain predefined threshold, the users are withholding their transmissions of mutual symbols until the channel conditions become more favorable. This precaution approach decreases the amount of useful TSs as well as the network throughput but would significantly improve the average BER performance by avoiding transmissions when the channel conditions are not favorable. Through this method, the worst cases are under control and have less effects on the overall BER performance. Here we assume that when an effective channel power gain is below a threshold, three users will all quit transmitting.

We have three ways to conduct the time scheduling, which will demonstrate the relationship between the throughput and the BER performance. The first method is that the three effective channel power gains are individually compared to the predetermined threshold and that users transmit messages only if all channel gains exceed the threshold. The *user pair*$_{13}$ and *user pair*$_{23}$ have rather low mean effective channel power gains, hence they will have a stronger possibility than *user pair*$_{13}$ to trigger the withdrawing process. However, any channel that does not satisfy the threshold will put all three users to sleep mode, and in this way, the BER performances of the three user pairs would still be different. For obtaining balanced results, the second method is to combine time scheduling with power allocation method when time scheduling is used first. Also, we can apply the power allocation first and then check if the evened effective channel power gain exceeds the threshold, which is the third method.

Different values for the threshold can be defined according to system performance requirements. For demonstration, we choose the threshold to be 0.0173 here, with the normalized system transmit power constrained to one, to examine the effective channel power gains. The simulation result for the first method is shown in Fig. 2.7 which illustrates the performance when only applying time scheduling. The BER results of *user pair*$_{13}$ and *user pair*$_{23}$ are improved around 10dB but *user pair*$_{13}$ has only 1dB improvement over the original scheme. This outcome is in accordance with the earlier analysis as the effective channel power gains of *user pair*$_{13}$ and *user pair*$_{23}$ have larger chances to be below the threshold, hence the time scheduling method would efficiently control the worst cases for both the user pairs and improve their

performances. However, this improvement is realized at the expense of a 24.75% reduction of the useful TSs for all users and the performances among user pairs are still different.

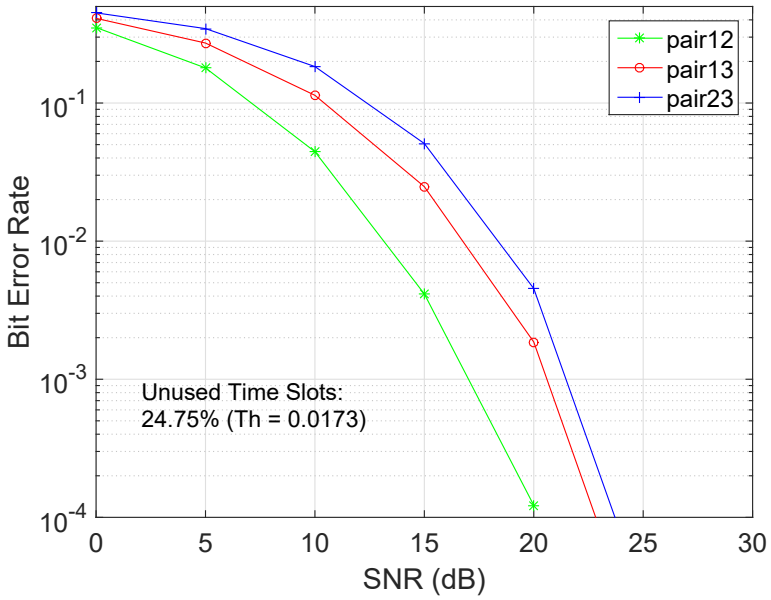

Figure 2.7: The BER performance of the proposed MIMO Y channel scheme with time scheduling.

Fig. 2.8 presents the relationship between the predefined thresholds and the corresponding loss in throughput when applying time scheduling. As seen in the figure, the relationship is linear.

Fig. 2.9 presents the throughput of the three user pairs when applying time scheduling and corresponds to the results in Fig. 2.7. The throughput versus SNR results is different for the three user pairs, same as it was the case for their BER performance. It is obvious that the throughput are decreased as compared to Fig. 2.5 for the original orthogonal signaling and the maximum throughput in this case is only about 0.75, a reduction of around 25% of the maximum throughput in Fig. 2.5. It should be pointed out that this reduction ratio is almost the same as the ratio of the unused TSs by conducting time scheduling. This is because when SNR is large enough and errors seldom occur, the throughput is basically equal to the transmit rate, but when a part of TSs are wasted without transmitting, the overall throughput must be reduced.

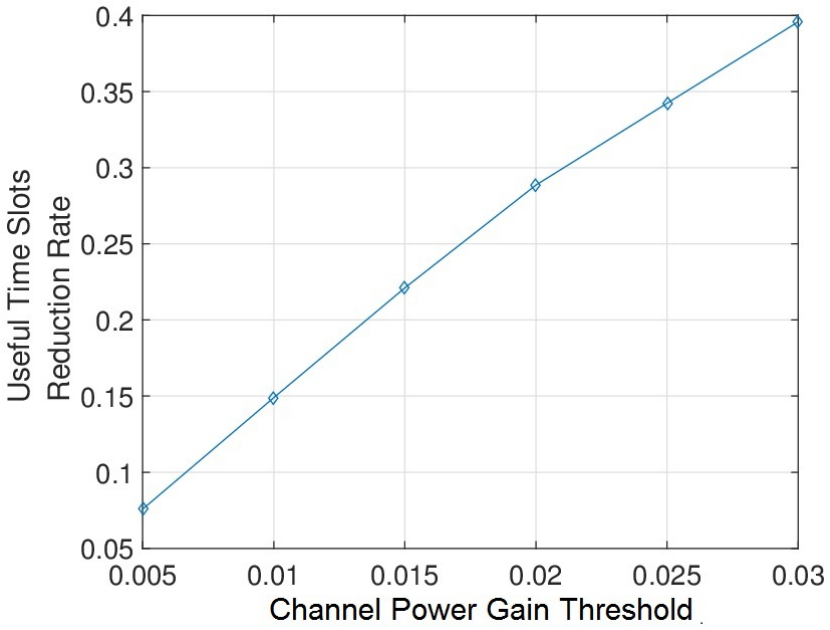

Figure 2.8: The relationship between the thresholds and the corresponding TS loss ratio in time scheduling.

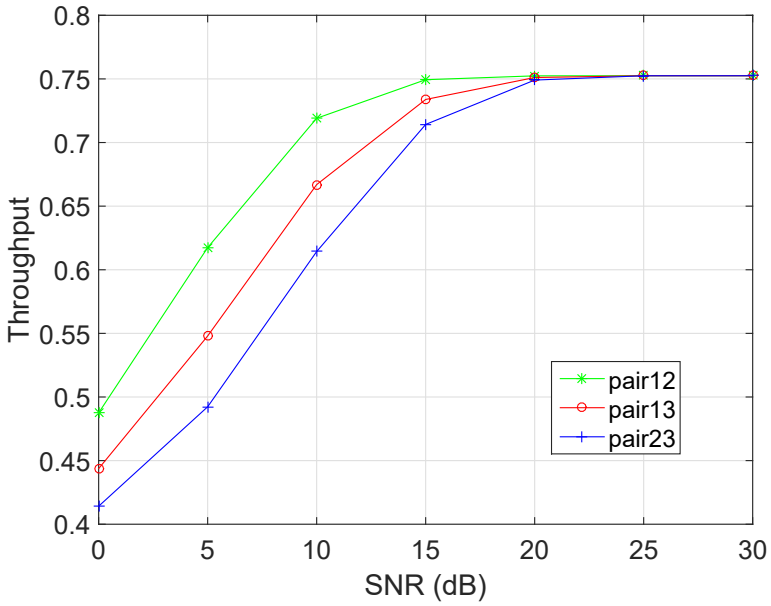

Figure 2.9: The throughput of the proposed MIMO Y channel scheme with time scheduling.

It is worth noting that the percentage of unused TSs is the same for any transmit SNR, since the predefined threshold used in the time scheduling is directly compared to the channel condition. This is reasonable for a system where power is crucial: when

a worst channel condition occurs, much larger transmit power or SNR is needed for offsetting the negative channel effects and achieving the same performance that a little power can obtain when the channel presents average condition. Hence, when power is of great importance, the system would not waste most of it to compensate for the worst channel condition. On the other hand, when power is not a great concern, the threshold should be compared to the instantaneous SNR where transmit SNR and channel conditions are considered simultaneously, which will be analyzed in Chapter 3.

Next we consider the performance of orthogonal signaling with power allocation applied after time scheduling to have balanced results for the three user pairs. The BER results for this shceme are demonstrated in Fig. 2.10. Two different predefined thresholds 0.0173 and 0.0035 are set here for affording comparisons. With the threshold 0.0173, the BER performances of the three users achieve BER 10^{-3} at 18.5dB with a cost of a 24.7348% reduction of useful TSs, while with the threshold 0.0035, for the same BER target, the SNR requirement is 23dB but only with a price of 5.2023% decrease of useful TSs. This outcome illustrates a tradeoff between the thresholds with the lost percentages of useful TSs and the BER performance: the higher the threshold is, which leads to the higher ratio of unused TSs, the better BER performance would be.

Finally, we analyze the performance of the third method, where power allocation is applied first and followed by time scheduling. For demonstration, we show the BER results in Fig. 2.11 with two thresholds 0.01 and 0.0378 for this case. It can be seen there that to get BER 10^{-3}, the SNR required is 23dB and 18dB for thresholds at 0.01 and 0.0378 with the drop of 5.8676% and 24.5884% of used TSs, respectively.

If we compare Fig. 2.10 and Fig. 2.11, the two figures are almost identical with respect to the associated unused TS ratios but not with respect to the thresholds. It seems that there is a clear relationship between the BER performance and the ratio of unused TSs, which is rather reasonable because unused TSs result in less errors and better BER performance. Therefore, the tradeoff to be exercised is between the useful TS reduction and the improved BER performance rather than the thresholds, and we can adjust either one to obtain the desired performance of the other one.

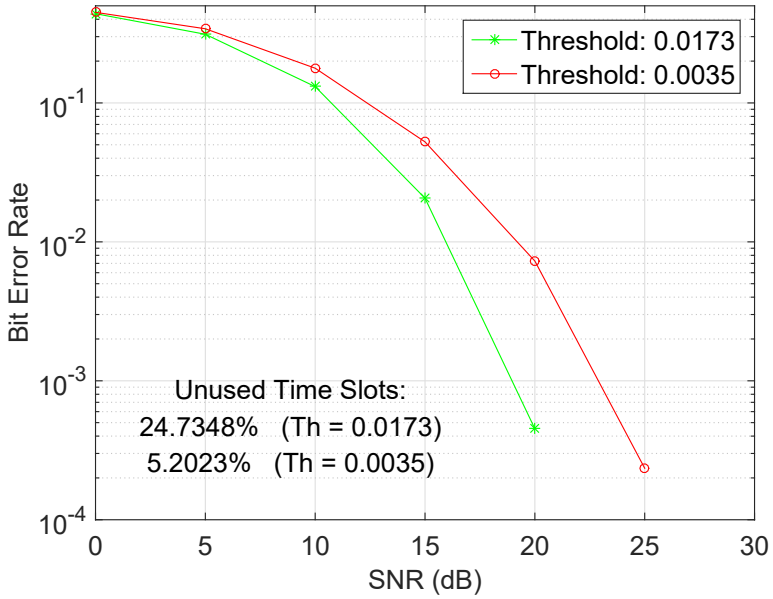

Figure 2.10: The BER performance of the proposed MIMO Y channel scheme with time scheduling applied first and then followed by power allocation.

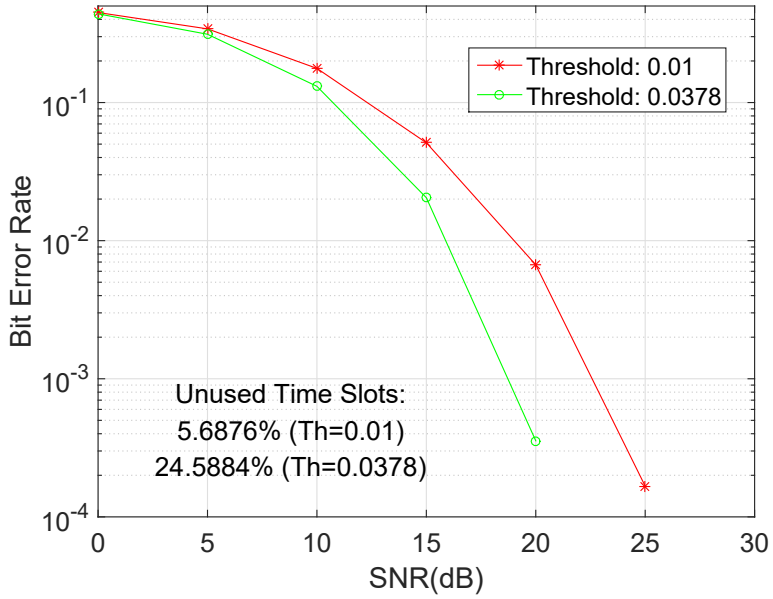

Figure 2.11: The BER performance of the proposed MIMO Y channel scheme with power allocation applied first and then followed by time scheduling.

As for threshold values for methods involving time scheduling, the larger threshold will lead to a larger ratio of lost TSs (i.e., TS not used for transmission). However, the method that uses time scheduling first always requires smaller thresholds than the method that applies power allocation first for achieving the same performance. For

instance, when the ratio is 25%, the threshold is 0.0173 for the second method and 0.0378 for the third method; when the ratio is 5%, the threshold is 0.0035 and 0.01 for the second and third methods, respectively. Hence, the sequence of applications of methods have influence on the thresholds. This is because, on one hand, when conducting time scheduling first, the threshold is used to judge every user pair's effective channel power gain. On the other hand, while using power allocation first, unacceptable effective channel power gain can be compensated from the redistribution of transmit power which results in the balanced effective channel power gain greater than the old worst gain of a user pair, and this increases the threshold in the time scheduling phase.

Fig. 2.12 presents the throughput comparison between the first method and the third method (the second method can have the same throughput results and BER performance with the same ratio of reduced TSs as the third method but with different thresholds). The figure shows the maximum throughput with the unused TSs percentage as the parameter.

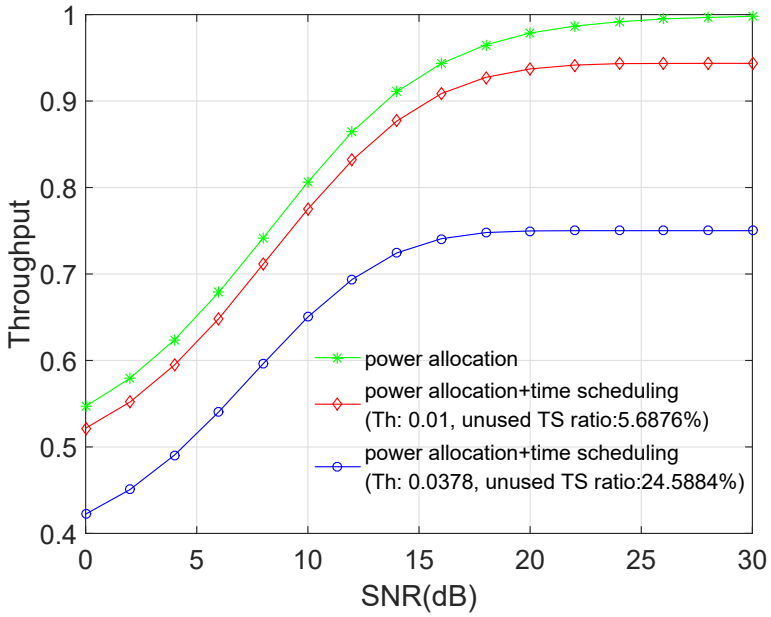

Figure 2.12: The comparison of the throughput in the scheme using power allocation and in the scheme using both power allocation & time scheduling with different thresholds.

To extract more information, we calculate the scale of the change in throughput caused by time scheduling using results from Fig. 2.12. The scales are shown in Fig. 2.13, where the vertical axis presents the reduced ratio of the throughput with the scheme applying time scheduling and power allocation to the one with only power allocation. In Fig. 2.13, the two curves first decrease and then rise to the percentages of unused TSs. The front drop means that the time scheduling can avoid bad TSs in the low-SNR regime when the effective channel gains are usually not desired, which diminishes the probability of occurrence of errors. However, when SNR is larger and errors seldom appear, the lost TSs will set a constraint to the achievable throughput in the system. This indicates that there is a minor relationship between the throughput and the SNR.

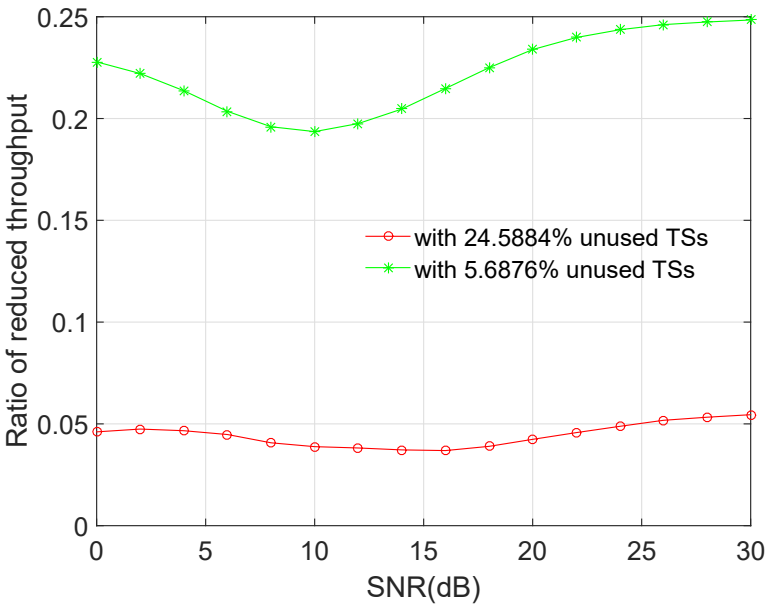

Figure 2.13: The ratio of reduced used TSs when applying time scheduling & power allocation compared to the one when applying power allocation.

2.4.3 Iterative Search for Optimized Orientation

The time scheduling method trades TSs for improvement in BER performance, and the results in Section 2.4.2 illustrate that combined with power allocation, the time scheduling algorithm can offer 14dB and 19dB improvements for all user pairs compared to the original MIMO Y channel, at the expense of 5.2% and 24.7% losses

of useful TSs, respectively. Moreover, we can further improve the BER performance and decrease the amount of unused TSs by employing iterative search for deciding the orientation of orthogonal signaling dimensions.

Because the unbalanced performance among three user pairs is caused by the preference given to user pairs in sequencing the steps to calculate precoding vectors, the proposed algorithm in this section uses six iterations that are generated by different sequences in solving the equation sets (1.3) and (2.1) for optimizing orientation of orthogonal effective channel gain. For example, we can calculate D_{12} first and then D_{13}, or calculate D_{13} first and then D_{23}, and there are total six permutations. Hence, in the algorithm, six sets of precoding vectors are independently calculated by iteratively solving six different ordered equations. Because the bottleneck of the system performance is the user pair with the worst result, we select the best set of precoding vector solutions which can offer the best effect on the worst user pair's performance. The selected sequence is actually random for each TS due to Rayleigh fading channels, and hence for a user pair the chances are equal to have the best, medium or the worst performance as exploited in the proposed orthogonal scheme. This randomization balances the three user pairs' performance, which is even better than the ones using power allocation that also intends to average the overall performance.

The simulation results with only iterative search for optimized orientation are shown in Fig. 2.14, providing almost 10dB improvement compared with the original MIMO Y channel. Also, the selection among six sets significantly reduces the level of the worst scenarios so that the overall performance using iterations is better than the one with power allocation as in Fig. 2.6. As the iterative search offers selections to utilize better the available signal space, it can be combined with the time scheduling to reduce the number of unused TSs. To compare the performance of this combined scheme with the results in Section 2.4.2, the same parameters for the third method in Section 2.4.2 are set for the simulations here and the outcomes are shown in Fig. 2.15. At BER 10^{-3}, the SNR is at 18dB and 21.25dB with thresholds 0.01 and 0.0378, respectively, and both provide 1dB improvement compared to the results without iterations in Fig. 2.11. What is more important is that the losses of used TSs in the scheme with iterations are reduced from 24.6% to 10.0% and from 5.7% to 1.8%, which

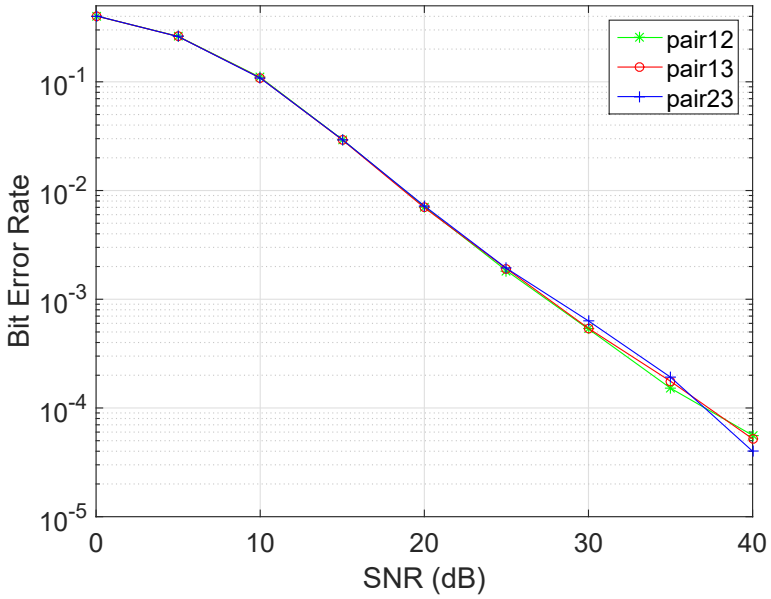

Figure 2.14: The BER performance of the proposed scheme with six iterations.

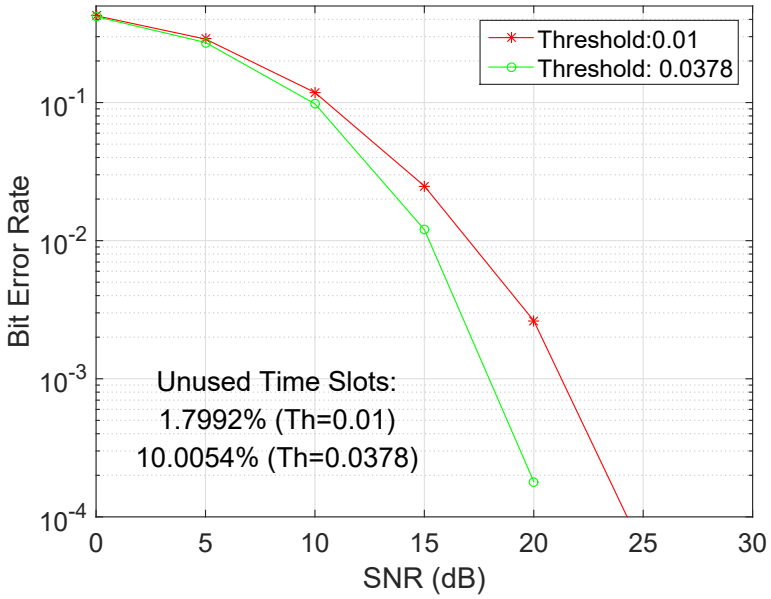

Figure 2.15: The BER performance of the proposed scheme with different applied methods.

is around a 60% saving of useful TSs. Therefore, the iterative search for orientation combined with time scheduling and power allocation can let more TSs be useful and even further improve the BER performance and throughput.

2.5 Conclusion

To compare the performance of different schemes and modifications in one place, we show in Fig. 2.16 the simulation results of balanced BER performance using schemes as identified in the legend of the figure. As seen in the figure, the power allocation alone gives 5dB improvement (at BER 10^{-3}) compared to the original MIMO Y channel scheme. Actually, the orthogonality provides different improvements for user pairs and the most improved one is 18dB. However, with power allocation, the user pair that has the best improvement redistributes much of its transmit power to compensate the worst user pair for a little improvement, but still the worst performance owns a larger weighting factor in the whole system outcome, finally leading to an average of 5dB improvement in the averaged performance.

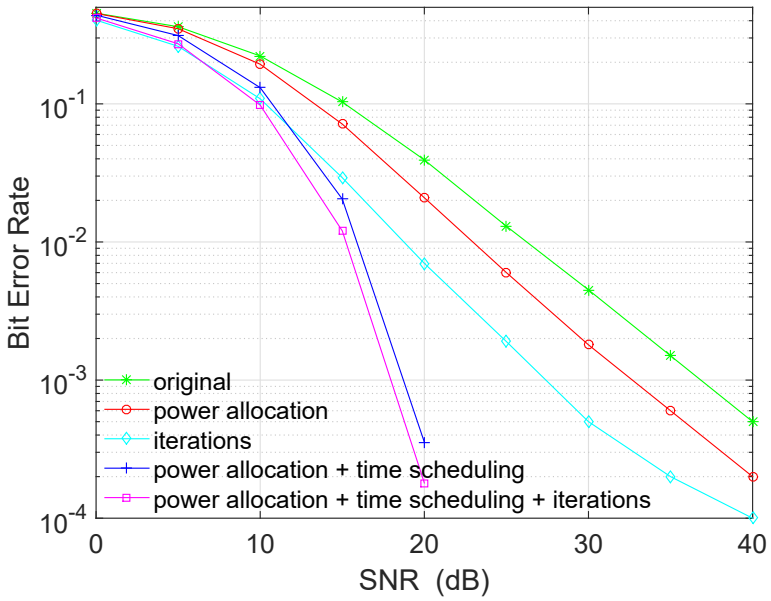

Figure 2.16: The BER performance of the proposed scheme with six iterations combined with power allocation and time scheduling.

For iterative seach only, the improvement is 10dB compared to the original scheme. Because of Rayleigh fading, the channel conditions are random, and hence if more selections are available and the best of them can be chosen, it would bring improvement for the BER performance. This method is utilized in some research papers such as in [16] and [18].

Next, when power allocation is applied with time scheduling, the worst cases are under control where users do not transmit messages when the effective channel gains are not favorable. This brings 18dB improvement for all users when compared with the original scheme but at a cost of a 24.6% reduction of useful TSs. The most significant property of MIMO Y channels is its high throughput where six packets are exchanged among three users in two TSs. However, using time scheduling, a perceived amount of throughput needs to be lost for BER performance improvement, and this would discount this major advantage. Hence, to reduce the lost of throughput and further improve the BER performance, iterative search is combined with time scheduling. In Fig. 2.16, when power allocation, time scheduling and six iterations are combined together, the BER performance is 19dB better than the original scheme and it only causes a 10% reduction of unused TSs. Compared to the results in [16] and [18] with the same antenna configuration as used in the proposed scheme and with the same target BER 10^{-3}, the best performance shown in Fig. 2.16 requires 9.5dB or 6dB less than in [16] where three or seven exhaustive iterations were conducted, respectively. [20] proposed a coding technique for the original MIMO Y channels and realized a coding gain of 23dB with a cost of a 75% reduction in throughput, but the scheme shown in this thesis only requires around 10% loss of throughput to achieve 19dB gain.

The orthogonality introduced in this thesis provides a simple way to perform the decoding in the MIMO Y channels without noise enhancement as in using ZF. However, it also introduces uneven BER performance for user pairs and this characteristic can be used in certain systems where there is a major communication link requiring better conditions than other links, as the improvement for the first user pair is tremendous. On the other hand, the signal space in the proposed scheme is not completely utilized as in the calculations for precoding vectors, several parameters are selected for simplicity. Therefore, the algorithm can be further improved with more sophisticated choices for those parameters and more restrictions for the aligned dimensions. The modifications are built under the condition that the balanced BER performance is required. Hence, even though it may be inefficient to apply power allocation, where much energy of the best user pair is sacrificed to compensate the worst user pair with a little improvement, this is achieved with low computational complexity. The six

iterations can also lead to the balanced performance for the three user pairs and even result in more BER improvement and a lower reduction of throughput, but the cost is the increased complexity of the algorithm.

Chapter 3

Bit Loading and Power Allocation

The previous chapter was focused on optimizing BER performance in MIMO Y channels with orthogonal signalling when BPSK was deployed at the terminal nodes. The current chapter applies the Gray-coded M-ary QAM in MIMO Y channels with orthogonal signaling to increase the throughput over the one bit per time slot in the MAC phase with BPSK for one user pair. While the M-ary QAM has been investigated for PNC [37] [38], this is the first application of M-ary QAM in the context of the MIMO Y channels with orthogonal spatial signaling. From the perspective of one user pair data exchange, when orthogonal signaling is deployed, the encoding with M-ary QAM is very similar to the conventional PNC with one spatial stream. However, in MIMO Y channel we deal with three spatial streams and new opportunities arise. Specifically, to optimize bandwidth and power resources in PNC in varying radio channels, data rate and power are adapted based on the channel quality. In this chapter, we apply rate and power adaptation in MIMO Y channel in a similar fashion as this was originally proposed for PNC but we do this across three spatial (parallel) streams corresponding to three user pairs.

This chapter is organized as follows. Section 3.1 discusses general ideas behind rate and power adaptations. Section 3.2 presents the system model where the MIMO Y channels can be treated as three parallel two-way relay channels. Next, Section 3.3 demonstrates the required knowledge to proceed the bit loading so that modulation levels are selected based on the effective channel gain. In Section 3.4, the sub-optimum bit loading with power allocation is added to the scheme to distribute transmit power and to select proper modulation types for each user pair for achieving the maximum throughput in the system. Finally, the simulation results are presented and discussed in Section 3.5.

3.1 Rate and Power Adaptations

In the previous chapter, the thresholds used in time scheduling in fading channels with BPSK are based on effective channel power gains which are the square of the absolute value of the multiplication of channel gains and precoding vectors, and not based on the instantaneous received SNR. The instantaneous SNR is the multiplication of the transmit SNR and the effective channel power gains, and it directly determines the BER performance. In this chapter, the rate and power adaptation is controlled by the instantaneous received SNR [39].

We show an example to demonstrate the difference between the power/thresholds decided based on (i) the effective channel gains and (ii) the instantaneous SNR. Assume a system (not necessarily with BPSK signaling) where the instantaneous SNR is required be ten to achieve BER 10^{-3} in a AWGN channel. Because AWGN channel coefficients are always one, the effective channel gains are always one, so that the transmit SNR is the same as the instantaneous received SNR. Therefore, the SNR and BER relationship in AWGN channels is the same as instantaneous SNR and BER relationship for fading channels. If this system intends to achieve the same BER in a Rayleigh fading channel, the required SNR is depended on the channel coefficients which vary in a wide range. For example, if at a moment the channel condition is bad and the channel coefficient is 0.1 (channel power gain is 0.01), the transmit SNR is required to be 1000 to let the instantaneous SNR be ten to achieve the aimed BER; if at one moment the channel coefficient of the Rayleigh fading channel is one (the average channel gain in Rayleigh fading channels), the transmit SNR is required to be 10 to achieve the aimed BER.

This example shows that when channel condition is bad, a significant amount of energy are required to compensate the negative influence caused by this channel for achieving the same performance that could only consume a little power when the channel is in its average status. Therefore, on occasions where the power efficiency is of great importance, users should decide whether to transmit according to the channel conditions. However, when it is not the case, users should send messages based on instantaneous SNR without consideration of the transmit SNR as long as the BER performance target is reached.

When users choose to transmit messages when channel conditions are acceptable, they can also determine the modulation level of symbols based on channel quality. More bits or a symbol with higher modulation level can be transmitted on a rather good channel and less bits or a symbol with lower modulation scheme can be transmitted on a rather bad channel, without influencing the BER performance. This is called bit loading. By using bit loading, the throughput of the transmission can be improved under a certain BER requirement. When the effective channel gain is sufficient for applying a higher modulation scheme to achieve a targeted BER, the system will use a higher modulation to increase throughput.

When there are multiple channels in a system, the transmit power for symbols on each channel can be redistributed to improve the whole system performance, e.g., the total sum rate. This is the bit loading with power allocation. The optimal one that reaches the capacity of the system with parallel channels is the water-filling algorithm. It allocates more power to messages on a good channel to support higher modulation, and stop sending messages in unacceptable bad channels. However, water-filling is more like a theoretical algorithm for channel capacity calculations where the bit assignment on any parallel channel can be any real number. This may be difficult to realize without designing integrated coding and modulation and this thesis is only considering the latter. There are also schemes like the Hughes-Hartogs algorithm which distributes power for maximizing throughput with discrete information bits determining feasible modulation scheme on parallel channels. The original Hughes-Hartogs algorithm for multicarrier transmission iteratively chooses the subcarrier that requires the least power to transmit one additional bit and allocates it with the exact amount of power needed. This method assigns the power with the aim to apply the highest modulation that the power can support under a certain BER requirement, so that the throughput is maximized with total power and BER performance constraints. In our proposed scheme, the Hughes-Hartogs algorithm is adapted to our conditions.

3.2 System Model

In this chapter, the system configuration is the same as the proposed one in Chapter 2, and channels are also assumed to be Rayleigh fading. As derived in (1.4),

in the MAC phase, the received signal at the relay is:

$$y_r = D_{12} \cdot (s_{12}) + D_{13} \cdot (s_{13}) + D_{23} \cdot (s_{23}) + n_r \tag{3.1}$$

Because of the orthogonality in (2.7), when the decoding process is conducted at the relay, the Hermitian transposed effective channel gain D_m ($m = \{12, 13, 23\}$) can directly multiply the mixed signal in (3.1) and one can decode the symbol s_m for the *user pair*$_m$ from the processed signal:

$$r_m = D_m^H \cdot y_r = D_m^H \cdot D_m \cdot (s_m) + D_m^H \cdot n_r \tag{3.2}$$

Then, when decoding an aligned symbol s_m, the instantaneous SNR for the channel with direction D_m is:

$$SNR_{instant,m} = \frac{|D_m|^2}{\sigma^2} \tag{3.3}$$

With this, the received signal in (3.1) can be represented in each orthogonal direction carrying one user pair's data as:

$$y_{r,m} = D_m \cdot (s_m) + n_{r,m} \tag{3.4}$$

where the noise components $n_{r,m}$ are also orthogonal and independent so that we could decode user pairs' data individually. Hence, the system model can be treated as three parallel two-way relay channels.

3.3 Bit Loading

In this thesis, we implement BPSK and Gray-coded M-QAM modulations in the proposed MIMO Y channel, as M-QAM are widely used in rate-adaptive communication systems. Specifically, we work at the user side with the modulation level M set either to 2, 4, 16 or 64 to limit the size of the expanded constellation at the relay (3, 9, 49 and 225, correspondingly). It should be noted that if ML decoding is directly applied, the relay need to evaluate 3^3, 9^3, 49^3 and 225^3 ideal points, correspondingly, but with the proposed scheme with orthogonal signaling dimensions, the decoding process is simplified to projecting the signal and slicing its coordinates along the dimensions, despite modulation levels.

The reminder of this section presents the necessary background for conducting bit loading and is organized as follows. Section 3.2.1 demonstrates the problem occurred

at the relay when conducting the encoding process with higher modulation levels and the corresponding solutions. Section 3.2.2 summarizes the thresholds for different modulations as they will decide the modulation level for each channel.

3.3.1 Constellation Mapping

In this section, we show that the constellation size at the relay is expanded and then how to perform decoding and encoding at the relay, so that in the BC phase, users could recover data of interest. We first demonstrate the details of the bit mapping process in the BPSK and 4-QAM modulation, and then present the problem that when using higher modulation schemes than the BPSK and the 4-QAM, the XOR encoding at the relay causes ambiguity. Finally, a solution is derived to resolve this ambiguity.

The constellation size at the relay is different from the applied modulation at users, as the received symbol at the relay is a superposed symbol of two symbols from two users. When the modulation level increases, the constellation size of the received symbol increases much faster. For symbols using BPSK of ± 1, the superposed symbols will have three levels: ± 2 and 0. Moreover, the 4-QAM leads to the received constellation of size 3×3 at the relay, because 4-QAM is a superposition of two BPSK along the in-phase and quadrature components. Furthermore, for 16-QAM the size of the received constellation at the relay is 49, and for 64-QAM the size is 225. Again this is because the 2-D M-QAM, where $M = \sqrt{M} \cdot \sqrt{M}$ is a superposition of two 1-D $\sqrt{M}$-ary PAMs along the in-phase and quadrature components. Generally, for square M-QAM at the user side, there is $(2\sqrt{M} - 1)^2$ aligned symbol at the relay on one spatial signaling dimension. This is because the received at the relay superimposed PAM in either in-phase or quadrature would be of size $2\sqrt{M} - 1$ [39]. If the relay was in the AF mode and it was resending symbols from the expanded constellations, this would result in the inefficient use of power for the aligned symbols, and moreover each user would have to decode two such aligned symbols. However, when the relay is in the DF mode, it can decode the received signals and re-map the symbols into a smaller constellation, which simplifies the decoding process for all users and results in the better use of power in the BC phase.

Now we show the mapping processes for different modulations at the relay. For BPSK, the mapping process is illustrated in Fig. 3.1 where the blue and red bits represent the information bits from two users and there are a total of 2^2 bit combinations, with two of them 01 and 10 resulting in the same aligned (superimposed) symbol decoded as 0 in the constellation. We can see it from the figure that the re-mapped constellation representing the XOR-ed version of user bits at the relay is still BPSK.

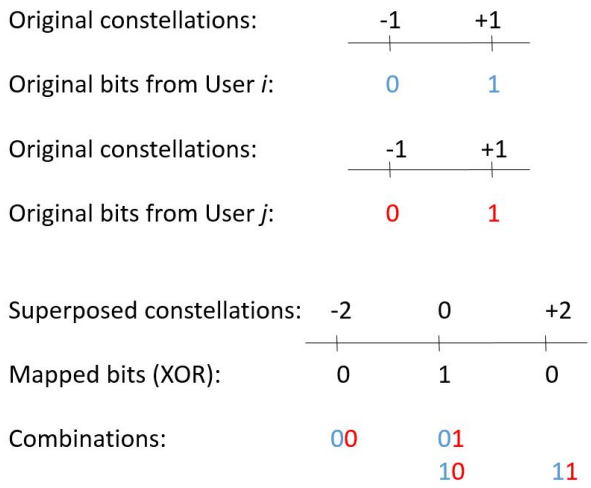

Figure 3.1: The decoding and remapping for BPSK symbols.

For 4-QAM, its in-phase and quadrature signals both can be considered as BPSK and hence the mapping for 4-QAM will be a 2-D BPSK mapping as shown in Fig. 3.2. The black dots are the aligned symbols of the yellow dots that are the original 4-QAM constellation. In each dimension, the yellow dots are at ± 1, and the aligned symbols are at ± 2 and 0 as in BPSK. The black bits represent mapped bits which are also the XOR-ed version of two users' bits.

So far, it seems that the re-mapping could be conducted following XOR of the original information bits. However, the XOR mapping can cause ambiguity when the modulation is higher than BPSK and 4-QAM [40]. Taking one dimension of 16-QAM, i.e., 4-PAM with two bits from one user as an example, Fig. 3.3 shows the ambiguity when trying to remap aligned 16-QAM symbols in one constellation dimension following the process as in BPSK. When the superposed constellation symbols are equal to $+2$ or -2, the XOR results of the gray-coded original symbols from two users are not unique. If the relay applies this mapping, users cannot decode their bits of interest.

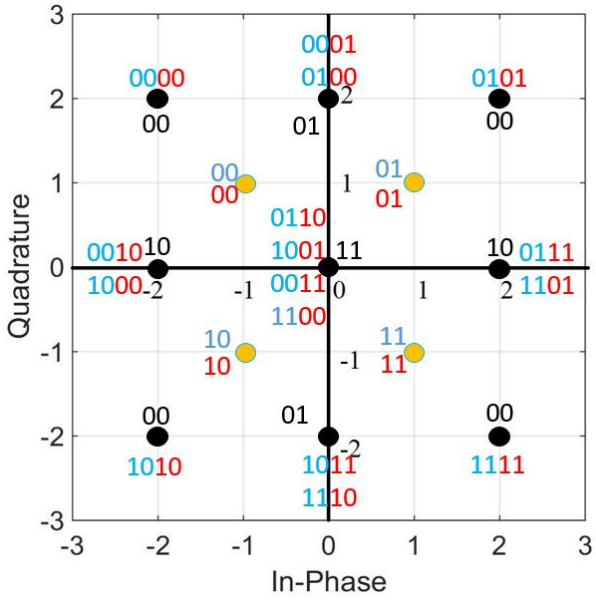

Figure 3.2: The decoding and remapping for 4-QAM symbols.

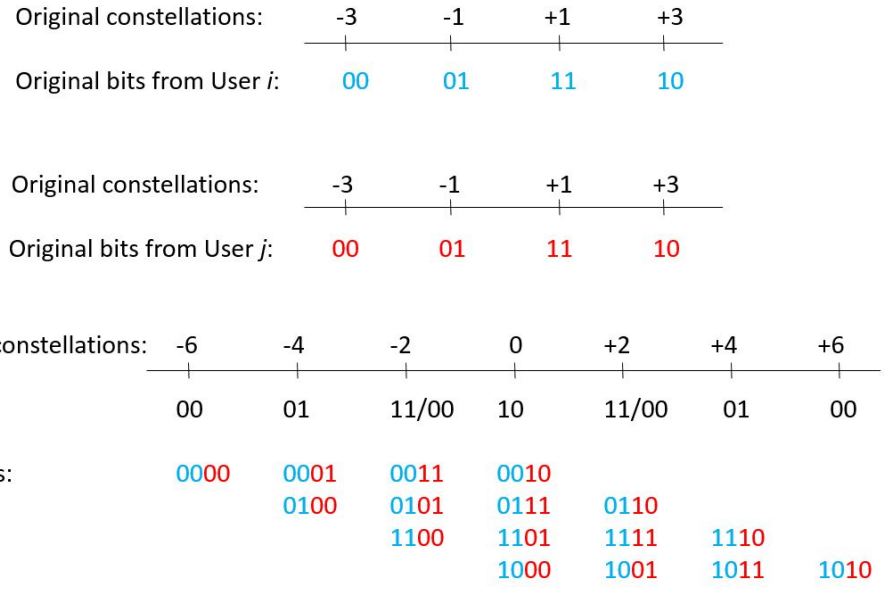

Figure 3.3: The ambiguity occurring in decoding and remapping for one dimension of 16-QAM symbols.

In order to avoid the ambiguity, we have to ensure that a mapping between a user's symbol and the aligned symbol is unique. In Fig. 3.3, the XOR result 01 representing constellation ± 4 and the XOR result 10 representing constellation 0, each has four combinations. In either group of these four combinations, the four blue information bits are different and the red bits are also different. This indicates that there is a

one-to-one relationship between the blue bits and the red bits under the XOR results 01 and 10 (which will allow recovery of data of interest at the user side in the BC phase assuming the user remembers its own data). Consequently, for the two remaining available mapping bits 00 and 11, each should also represent four combinations, despite XOR results, with a condition that in the group of four combinations the blue and the red information bits need to have one-to-one relationship. For instance, if the mapping bits 00 represent constellation -6 to have the combination 0000, it cannot represent -2 because there is a combination of 0011 where 00 is repeated with the blue bits in the former combination 0000. One possible mapping that satisfies this rule is shown in Fig. 3.4.

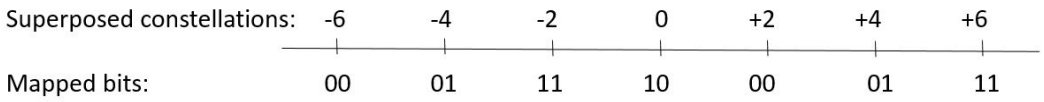

Figure 3.4: The decoding and remapping of 4-PAM symbols corresponding to 1-D in 16-QAM signalling.

Table 3.1: The bit mapping for the combination of two 4-PAM symbols.

Mapped Bits	00	01	11	10
Bit Combinations of Two Symbols Individually from Two Users	0000	0001	0011	0010
	0110	0100	0101	0111
	1111	1110	1100	1101
	1001	1011	1010	1000

In addition, corresponding to Fig. 3.4, the mappings of the combinations of two original symbols are summed up in Table 3.1. It can be seen that under each group of the mapped bits, if a symbol in blue or red is known, the other symbol can be decided. For instance, an aligned symbol is remapped to bits 11, and this remapped symbol is sent to users; if the blue user receives bits 11 and knows its former transmitted bits are 11, it can decode the desired bits 00 from the red user according to Table 3.1. This one-to-one mapping between two original symbols under a mapped symbol at the relay provides a look-up table for users without ambiguity. XOR mapping can still be used for simplicity where no uncertainty occurs. Wang *et al*. proposed a mapping algorithm involving modulus [40], but our method is simpler and faster via a direct mapping table for each modulation scheme.

3.3.2 Modulation Thresholds

In this section, we derive the thresholds for determining modulation levels for each of the three spatial channels in our system model with orthogonal signaling. To obtain the thresholds, we need to determine the targeted BER and the BER performance of the superposed symbols received at the relay. Moreover, because the instantaneous $SNR_{instant,m}$ in fading channels has the same effect one the BER performance as in AWGN channels, the BER performance of different constellations for those superposed symbols in AWGN channels will be obtained and used to determine modulation levels for the proposed scheme in Rayleigh fading channels.

In this thesis, we aim at the BER 10^{-3}, and the corresponding thresholds when switching between different modulations based on SNR can be determined from Fig. 3.5, which shows the BER as a function of the received SNR (per superposed symbol) for different modulation levels of the received symbols at the relay. The bit

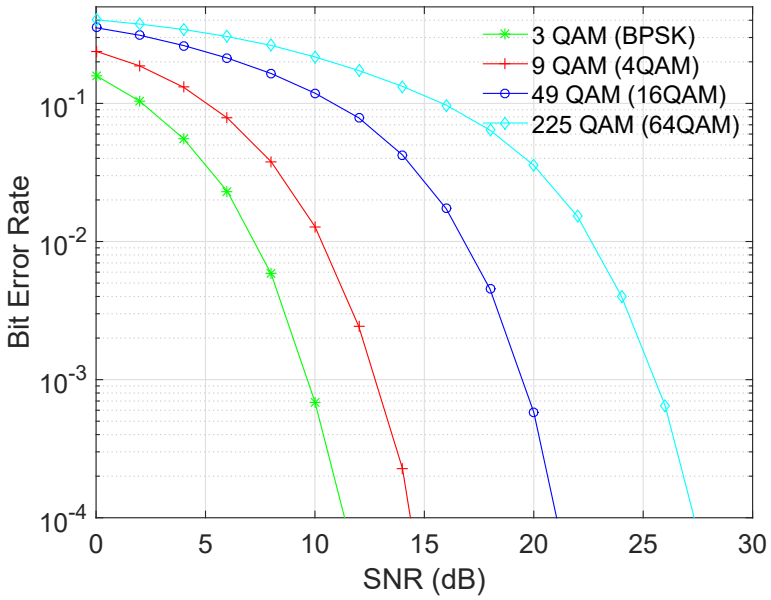

Figure 3.5: The BER performance of the received symbols at the relay with different modulations in AWGN channels.

error rate performance for the superposed constellations is analyzed in Appendix A, where we reach the conclusion that the bit error rate performance of the superposed constellations at the relay is 3dB worse than that of the original constellation at the user sides. Therefore, to obtain the plots in Fig. 3.5, we could use the readily available

expressions for the conventional QAM constellations used at the user sides with the appropriate shifts [28]. The thresholds for the SNR at the relay to decide when to switch between different original constellations at the user sides are summarized in Table 3.2. As a side note, these thresholds are related to the SNR at the transmitter which is used when analyzing the performance of our system in the simulation section.

Table 3.2: The modulations and the corresponding thresholds for achieving the aimed BER 10^{-3}.

Modulations	Thresholds	Range
NO TX	—	0 dB $<$ SNR $\leq$ 9.9 dB
BPSK	9.9 dB	9.9 dB $<$ SNR $\leq$ 12.9 dB
4-QAM	12.9 dB	12.9 dB $<$ SNR $\leq$ 19.7 dB
16-QAM	19.7 dB	19.7 dB $<$ SNR $\leq$ 25.7 dB
64-QAM	25.7 dB	25.7 dB $<$ SNR

3.4 Sub-optimal Power Allocation

Since we determined the thresholds for deciding among modulation levels for each channel and managed to create a practical bit encoding algorithm at the relay, we can implement the bit loading. On the other hand, we can also distribute power with careful calculation to users to obtain the most power efficiency in pursuing the maximum throughput.

As discussed earlier, the water-filling algorithm is the known optimal method to allocate power, but the bit distribution obtained can be any real number, which is difficult to implement in practice; while the Hughes-Hartogs algorithm is based on discrete information bits or a finite granularity, and is used in this thesis for it being a classic optimum bit loading algorithm in literature [33] [41].

For a multi-channel transmission system, the Hughes-Hartogs algorithm, based on the greedy optimization approach, iteratively assigns one bit to a subcarrier that requires the least transmit power with the constraints of total power and a BER target. The meaning of "greedy" here is that the power is allocated with the goal to send more bits in the system. Hence, subcarriers only obtain the exact amount of power to achieve the BER required for their modulation level transmission, and any extra power is collected for possible increase of modulation levels for other subcarriers.

The original Hughes-Hartogs algorithm assigns one bit at one time, however in our system, the selected modulation types are BPSK, 4-QAM, 16-QAM and 64-QAM, where the bit increment is one from BPSK to 4-QAM and is two between other neighboring modulations. Therefore, the Hughes-Hartogs algorithm is revised to suit our scheme.

3.4.1 Sub-optimal Power Allocation

In this section, we demonstrate the process for performing the sub-optimized power allocation for achieving better throughput. The power distribution is feasible through the control of precoding vectors as discussed in Section 2.2. To reallocate transmit power among users with the target BER, we need to add different constraints on precoding vectors with the total power limit. Refer to the transmit power constraint in (1.2), and when we add parameters to adjust the power among precoding vectors, it is transformed into:

$$x \cdot (|v_{21}|^2 + |v_{12}|^2) + y \cdot (|v_{31}|^2 + |v_{13}|^2) + z \cdot (|v_{32}|^2 + |v_{23}|^2) = \frac{x}{3} + \frac{y}{3} + \frac{z}{3} = 1 \quad (3.5)$$

with

$$x + y + z = 3 \quad (3.6)$$

where x, y and z are the power allocation parameters to achieve the sub-optimum discrete bit loading for the proposed scheme and (3.6) will guarantee the total transmit power remains one. Then, the adjusted $SNR_{instant,m}$ for each user pair is $x \cdot SNR_{instant,12}$, $y \cdot SNR_{instant,13}$ and $z \cdot SNR_{instant,23}$, respectively.

Now we have the parameters representing the allocated power for each user pair with the total power limit, and we will proceed with development of the sub-optimum bit loading with power allocation are as follows. First, the thresholds for using each modulation with a target BER need to be defined. The target BER is still selected to be 10^{-3}, and then the thresholds used here are identical with the ones in Table 3.2. Next we calculate the power that is required for each user pair with their original $SNR_{instant,m}$ to achieve the BER performance using varying modulation levels as:

$$p_{m,n} = T_n / SNR_{instant,m} \quad (3.7)$$

where $n = \{1, 2, 3, 4\}$ represents BPSK, 4-QAM, 16-QAM and 64-QAM, respectively, and $p_{m,n}$ is the relative power needed compared to $SNR_{instant,m}$ with nth modulation and T_n is the SNR threshold to achieve the BER target with nth modulation scheme.

Table 3.3: The relative power required for achieving the aimed BER 10^{-3} using each modulation scheme compared to the current transmit power for each user pair.

-	$SNR_{instant,12}$	$SNR_{instant,13}$	$SNR_{instant,23}$
BPSK	$p_{12,1}$	$p_{13,1}$	$p_{23,1}$
4-QAM	$p_{12,2}$	$p_{13,2}$	$p_{23,2}$
16-QAM	$p_{12,3}$	$p_{13,3}$	$p_{23,3}$
64-QAM	$p_{12,4}$	$p_{13,4}$	$p_{23,4}$

Table 3.3 lists the ratio of required transmit power to achieve the BER aim with a certain modulation level and the current transmit power. When $p_{m,n}$ is greater than one, it states that the channel with $SNR_{instant,m}$ needs more transmit power to reach the BER aim with nth modulation; when $p_{m,n}$ is smaller than one, it shows that the $SNR_{instant,m}$ is greater than the power that this modulation is required to achieve the BER target, and hence extra transmit power can be collected to be redistributed to a subcarrier that is closest to its next modulation level. For example, when $SNR_{instant,13} = 8$, $p_{13,1} = T_1/SNR_{instant,13} = 6.9/8 = 0.8625$, which means that only 86.25% power of the precoding vectors v_{13} and v_{31} are required to use BPSK to achieve BER 10^{-3}; $p_{13,3} = T_3/SNR_{instant,13} = 16.7/8 = 2.0875$ means that 2.0875 times the present power of precoding vectors v_{13} and v_{31} are needed to apply 16-QAM modulation with target BER 10^{-3}.

The power parameters in Table 3.3 are obtained by comparing with the subcarriers' original $SNR_{instant,m}$, which states the power required for each individual modulation, but when the subcarrier intends to jump to a higher modulation level, the power needed is the subtraction of the power parameter of the current modulation level from the power parameter of the new modulation level, which can be indicated as the relative required power between modulation levels. Consequently, Table 3.3 is transformed into Table 3.4.

Finally, the minimum parameter from the set $\{x_a,\ y_b,\ z_c\}$, $(a = b = c = 1$ at initial; $a, b, c \in \{1, 2, 3, 4\})$ is selected and the index of the selected parameter

Table 3.4: The relative power required for achieving the aimed BER 10^{-3} using next modulation level compared to the current modulation scheme for each user pair.

-	$SNR_{instant,1}$	$SNR_{instant,2}$	$SNR_{instant,3}$
BPSK	$x_1 = p_{1,1}$	$y_1 = p_{2,1}$	$z_1 = p_{3,1}$
4-QAM	$x_2 = p_{1,2} - p_{1,1}$	$y_2 = p_{2,2} - p_{2,1}$	$z_2 = p_{3,2} - p_{3,1}$
16-QAM	$x_3 = p_{1,3} - p_{1,2}$	$y_3 = p_{2,3} - p_{2,2}$	$z_3 = p_{3,3} - p_{3,2}$
64-QAM	$x_4 = p_{1,4} - p_{1,3}$	$y_4 = p_{2,4} - p_{2,3}$	$z_4 = p_{3,4} - p_{3,3}$

increases by one each time to represent the power parameter for the next modulation level. The process repeats until the sum of all selected parameters reaches the total transmit power limit. The final subscripts of x, y and z indicate the modulation the corresponding channel should use. If there is a little power left and this amount of power cannot support any channel to upgrade modulations, it will be evenly divided to all carriers to boost their performance with the modulation they can apply.

3.5 Simulation Results

In this section, we demonstrate the simulation results for bit loading and the sub-optimum power allocation with the target BER 10^{-3} in the MIMO Y channel with orthogonal signaling. We implement the iterative search for optimized parameters to achieve better throughput while maintaining acceptable BER and balancing the three users' performances. Fig. 3.6 (a) shows the BER for the scheme with bit loading, while Fig. 3.6 (b) presents the BER for the scheme with the integrated bit loading and power allocation. Moreover, Fig. 3.7 illustrates the throughput results associated with Fig. 3.6. Again throughput in this thesis is measured in successfully transmitted bits per time slot for one user pair.

In the lowest SNR regime, the BER in Fig. 3.6 (a) for all users are not meeting the targeted level so there are no results/lines in this region. The target BER is always met when SNR is above 10dB. When SNR is between 7.5dB and 15dB, the BER shows differences for three users, which seems to be against the fact that our iterative search is attempting to balance the three users performances. The reason is that the low SNR in this case causes low throughput, so that the simulation results may not be as accurate as the ones in higher SNR. Fig. 3.7 demonstrates that in the low SNR regime between 0dB and 10dB, the throughput of bit loading is almost zero,

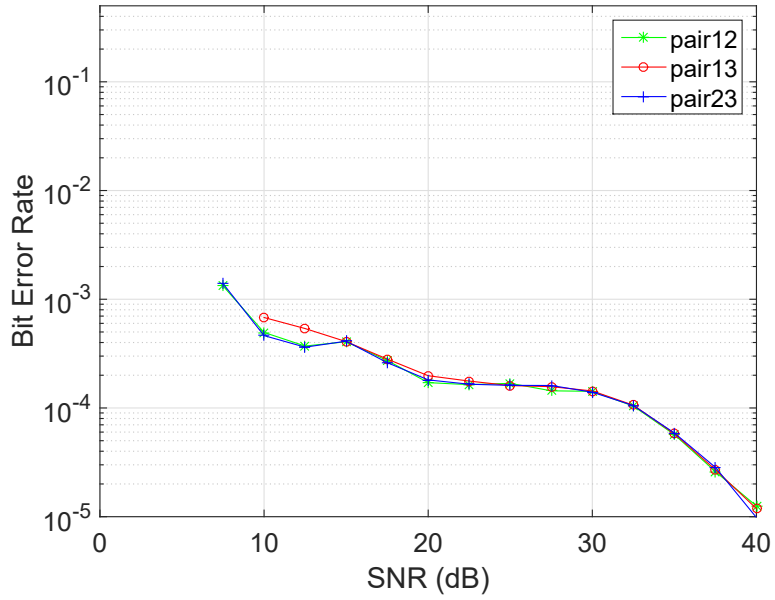

Figure 3.6: The BER comparison between the system with (a) the bit loading and the integrated bit loading and (b) power allocation.

while the throughput of the bit loading with power allocation increases from zero to around 0.37.

With SNR above 15dB, the bit loading with power allocation (Fig. 3.6 (b)) has worse BER performance than the bit loading (Fig. 3.6 (a)) . As we indicated in Section 3.3, if the obtained BER is better than the target, the extra power can be

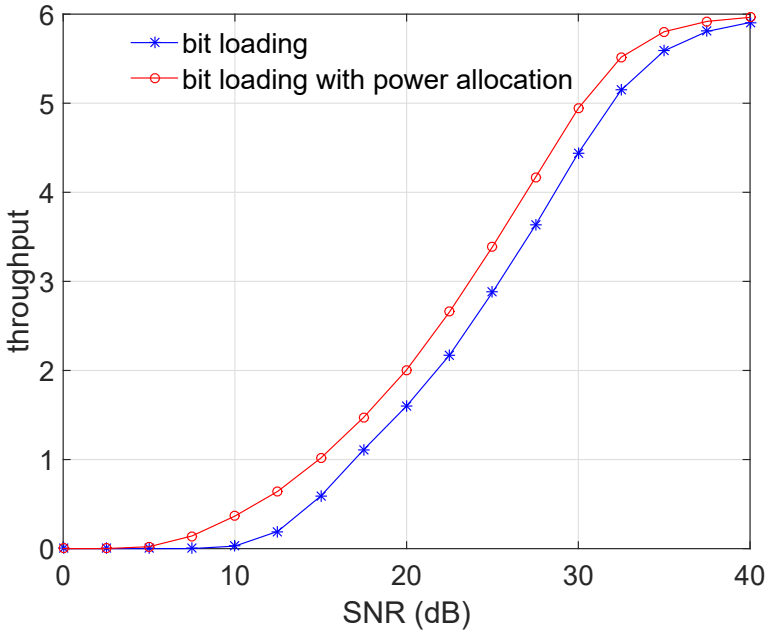

Figure 3.7: The throughput comparison between the system with the bit loading and the integrated bit loading and power allocation.

collected and distributed to parallel (spatial) streams which can offer higher throughput. This is corroborated in Fig. 3.7 where the throughput of the bit loading with power allocation is indeed better than that for the bit loading alone. This reinforces the statement that the bit loading with power allocation assigns power and bits more efficiently by achieving better throughput while meeting the BER constraint.

However, when SNR is around 40dB, BER in Fig. 3.6 (b) and in Fig. 3.6 (a) are close to each other. Due to such high SNR, the selected modulation for either case is usually the available highest one, 64-QAM. This implies that, in the bit loading with power allocation, power cannot be used to further upgrade modulation levels for any subcarrier anymore but can be used to boost the BER performance with current modulation levels for each subcarrier. Fig. 3.7 also shows that the two methods nearly reach the highest available throughput around 40dB of $\log_2(64) = 6$ bits. However, we can see that the bit loading with power allocation offers higher throughput than the bit loading in the SNR regime in Fig. 3.7. Therefore, the proposed bit loading with power allocation in the MIMO Y channel is an efficient way to allocate power to improve the throughput and boost the BER performance compared to bit loading alone.

It is worth mentioning that the Hughes-Hartogs algorithm can have better throughput performance than its modified version in this thesis, as the power allocation in the Hughes-Hartogs algorithm is considered bit by bit, while in the proposed scheme, the bit increment is different in the selected modulations BPSK and M-QAM, which sometimes may cause inefficient power allocation for improving throughput. For instance, there is a subcarrier requiring power a to transform from BPSK to 4-QAM and another subcarrier requiring power b to transform from 4-QAM to 16-QAM. If $b > a$, the proposed algorithm would choose the first subcarrier, but if at the same time $a > \frac{b}{2}$, this selection may not be the most efficient as the second subcarrier needs less transmit power per bit. However, the selection can be seen as the one that the system tries to encourage all user pairs to transmit even though they are using BPSK. Therefore, although the Hughes-Hartogs algorithm is better than the proposed scheme in maximizing the system throughput with the power allocation considered bit by bit, the proposed algorithm is much simpler with less iterations and offers sub-optimal power and bit allocation. Moreover, the system only needs to implement the common BPSK and M-QAM encoders and decoders rather than complex ones for the original Hughes-Hartogs algorithm.

Chapter 4

Conclusion

In this chapter, an overview of the thesis contributions and suggestions for future work are presented. Section 4.1 discusses the contributions of this thesis and Section 4.2 suggests the future work.

4.1 Thesis Contributions

There are two main contributions in this thesis that pertain to improving the reliability and throughput in MIMO Y channels.

The first contribution is the introduction of orthogonality to the selection of aligned signal dimensions, which simplifies decoding processes at the relay. It also improves the BER performance for the three user pairs with BPSK signalling. However, the initial approach suffers from the unbalanced BER performance among different users. To alleviate the problem and improve BER performance further, different modifications in the original orthogonal signal alignment scheme were developed.

The second contribution is in incorporating higher level QAM modulation schemes into MIMO Y channel signaling with orthogonality. Specifically, the bit loading with power allocation in MIMO Y channels was developed to distribute power and to assign modulation levels on parallel spatial streams with the goal to increase the system throughput.

In the area of the first contribution, by working with redundant antennas at the user terminals, this thesis proposes to constrain the aligned signal dimensions to be orthogonal. Computationally efficient method was developed to calculate the precoding vectors. The orthogonality simplifies the decoding process at the relay offering the performance of the minimum distance ML decoding. By projecting the received signals and slicing them along three orthogonal directions, the receiver complexity is lower than that of the ZF decoder which requires matrix inversion, and the proposed scheme does not suffer from noise enhancement caused by ZF. Moreover, when higher

modulations are used at users, the proposed decoding process still has the same computation complexity as when users use BPSK, while applying ML decoding directly can be very complex due to the size of the superposed constellation at the relay, e.g., 225^3 calculations of distance are required at the relay when users use 64-QAM. Hence, the simplification of decoding process from the proposed scheme is of great importance using higher modulations. In addition, as all user nodes and the relay node have the same antenna configuration in the proposed system, each node can perform as a user or a relay. Hence, the system can be part of ad hoc networks, or the multiple systems can constitute an ad hoc network.

In the area of the second contribution, this thesis presented first the process of bit mapping in QAM constellations used at the terminals in the MAC phase in order to recover the mutual bits in the expanded constellations at the relay, so that these mutual bits could be re-encoded in a reduced-size (original) constellation in the BC phase. Because of the constellation expansion at the relay, e.g. from $16 = (4 \times 4)$ QAM to $49 = (7 \times 7)$ QAM, there was a need to carefully design the bit assignment to minimize the impact of symbols in error, in a similar way that the Gray encoding accomplish this objective in the conventional modulation schemes. Once the higher level QAM processing was established, a method of distributing bits and power allocation among the spatial streams was developed by working with discrete bit allocation algorithms similar to those used in multicarrier modulation systems.

Specific problems and detailed solutions of the first contribution are summarized as follows:

1. Precoding Vector Design for MAC Phase

First, the precoding vectors as in the signal pre-processing at the terminals need to satisfy the SA requirement to put the mutual symbols from two users in one signal dimension. If doing so with the minimum configuration of antennas, there is only one eligible signal dimension for one pair of mutual signals. The obtained aligned dimensions and the effective channel gains for aligned symbols are only SA constrained, which leads to the situation that the Euclidean distance between neighboring aligned symbols varies within a large range. The SER performance in the communication systems is limited by the worst case; therefore, as long as the distance between symbols

appears to be small (even occasionally), the whole BER performance will be influenced badly. In order to provide control of the aligned dimensions, in this thesis, each user terminal is equipped with one redundant antenna, which brings more diversity gain that can afford to satisfy additional signal dimension requirements such as to maximize the distances and to improve reliability. We also include the orthogonality as one of the conditions to select precoding vectors so that the decoding at the relay can be simplified by projecting received symbols on the three orthogonal dimensions and thresholds. Using original ML decoding (which calculates the Euclidean distances between the received signal and ideal symbols) may become complex for higher modulation levels. Our design was actually motivated by simpler implementation of the ML receiver by sacrificing some performance loss (in terms of BER), as a result of using hyper-cube constellation of points and higher number of antennas. Computationally efficient method was developed to calculate the precoding vectors with the orthogonality constraints, however, the method introduced unbalanced BER performance among different users which had to be addressed as discussed next.

2. Modifications and Improvements with BPSK Orthogonal Signalling

The BER results from the proposed MIMO Y channel are not balanced for the three user pairs due to the preference in the sequence of solving the sets of equations, i.e., constraints. In order to have even performance for all users, two methods are applied: one is the power allocation where the transmit power of the user pair with better BER is reallocated to compensate the user pair with worse BER; the other one is the iterative search by solving the equation sets in six different sequences of steps. In the iterative search, the outcome which offers the best performance for the worst user pair/link is selected from the six sets of solutions to mitigate the worst scenario. Then, the obtained assignment of effective channel power gains for different user pairs is randomized, which can balance the BER of the three user pairs. Next, to further improve the BER performance, an efficient approach called time scheduling is proposed where users stop transmitting if the channel condition is not acceptable. This method aims to avoid the worst scenarios by users stopping transmitting messages in such situations. A small amount of throughput would be lost, but BER is significantly improved. Moreover, when iterations are combined with time scheduling, the reduction in throughput of the proposed system over the original

MIMO Y channel is not that significant while achieving the targeted BER.

Contributions in the second part of this thesis are as follows:

1. Deployment of Higher Level QAM Modulations

We propose a mapping strategy for using higher modulations in SA. Deployment of BPSK at the terminals results in the need for ternary signal detection at the relay (in each spatial dimension) and the proper interpretation of received signals as the XOR-ed version of mutual symbols. Since the QPSK can be considered as two independent BPSK modulations along the in-phase and quadrature components, the generalization of BPSK into QPSK is rather straightforward. In our approach, $M = (L \times L)$ QAM at the terminal is a superposition of two L PAM signallings along the in-phase and quadrature components. When combining two L PAM mutual symbols (in each spatial dimension), at the relay we had to detect $(2L-1)$ PAM (in both in-phase and quadrature dimensions), which is equivalent to ternary symbols when $L = 2$, i.e., when we deploy BPSK. It is this observation that led us to work with the expanded $M' = (2L-1) \times (2L-1)$ QAM constellations at the relay and the need to the bit mapping so that we could recover the mutually bits. However, when L is greater than 4, the mutually bits cannot be mapped to their XOR results due to ambiguity. Hence, we propose the mapping strategy that can cancel the ambiguity with low computational complexity.

2. Bit Loading in the Spatial Channels

In this area of our research, we implement the bit loading with power allocation in the MIMO Y channels. The algorithm offers the system the capability of changing among modulation schemes on three spatial (parellel) channels and allocating power to achieve a higher bit rate, with constraints of total power and target BER. The bit loading with power allocation used in this thesis is adapted to the underlying system from the Hughes-Hartog algorithm. In the proposed scheme, the number of assigned bits in each iterative assignment is not the same, while in the Hughes-Hartog algorithm which offers optimized throughput, the number is the same. The proposed algorithm offers sub-optimal performance but is simpler with less iterations than the Hughes-Hartog algorithm, and a system only needs to implement BPSK and M-QAM encoders and decoders to use the proposed algorithm.

In summary, the contributions of this thesis are obtained by exercising the tradeoff

among system complexity, computational complexity, system reliability, bandwidth efficiency and power efficiency. In the original MIMO Y channel, the bandwidth efficiency is the most noteworthy advantage, but the BER performance is lacking even in a high SNR regime. In the proposed schemes, some degradation in throughput can be traded off for significant improvement in BER. Specifically, in Chapter 2, after introducing precoding vectors for orthogonal spatial signaling, the iterative search for balancing user pair BER performance is combined with time scheduling to reduce the throughput loss, but this introduces higher computational complexity in obtaining precoding vectors. Moreover, the adaptive modulation introduced in Chapter 3 leads to higher throughput with a targeted BER by efficiently allocating power and bits, but again the system implementation is more complex.

4.2 Suggested Future Work

The potential for future work is discussed in this section.

As in any new cooperative communication scheme, there are some generic problems such like how to handle the effects of imperfect CSI and synchronization, and there are some issues specific to our schemes. Even more pressing issue is that our work is at the theoretical level verified with simulations so it is natural to ask about feasibility of practical applications. To address the latter concern, there are already some practical verifications of SA schemes using a real-world communication testbeds that demonstrate that the observed gains of SA in the practical settings are in accordance with the theory and simulation results [42].

A few topics related to the present study are suggested as follows.

1. Effects of Imperfect Channel Information

In MIMO Y channels, the perfect CSI is assumed to be available to all nodes, as users and the relay need global channel conditions to calculate proper precoding vectors to implement SA. However, in practical applications, CSI is normally gathered through receiver estimation and transmitter feedback, which would cause the delay and inaccuracy of CSI at user nodes. This thesis does not consider this situation, but this problem has been studied by many researchers in other settings by analyzing performance with imperfect CSI and proposing new algorithms to mitigate this issue [43]–[45].

2. Precoding Design for BC Phase

In this thesis, we only discuss the MAC phase for precoding designs in the proposed scheme, and for the BC phase we assume that the nulling vectors can be obtained with antenna selection. However, more detailed investigation can be pursued to exploit the possibility of improvements in the BC phase.

3. Synchronous Transmissions

SA is about aligning two symbols, or equivalently two synchronous signals, in one signal dimension at the relay where the addition of synchronous signals is through the over-the-air summation. The problem is that sometimes it is not sufficient to be synchronized when sending the data because the requirement is for synchronous reception. In that case, users are required to coordinate with each other through network protocols and other methods with regard to their locations, which are not studied in this thesis. However, this issue can be solved with OFDM technology where the symbol rate is very low in each subcarrier so that the delay over different user paths to the relay can be neglected. In our work, we were also assuming that all users have the data to be sent at all the time, which may not be the case for asynchronous traffic. This may be solved through different buffering strategies.

4. Path Loss Considerations

Deterministic path loss (or path attenuation) is the reduction in power of an electromagnetic wave as it propagates through space over given distance. In this thesis, we did not consider deterministic path loss, i.e., the distances between each user and the relay are assumed to be the same. However, in reality, the distances are normally not the same, and the attenuation of signal power is related to the link distance. Therefore, to let the two mutual signals have the same power weight in the aligned signal dimension for achieving higher decoding accuracy rate, the distances between users and the relay should be considered for power allocation.

5. Bit Loading with Power Allocation

The proposed bit loading algorithm provides the sub-optimal solutions because it does not consider the most efficient power and bit allocation as the Hughes-Hartog algorithm does, where the incremental bit unit is one between neighboring modulations. However, the proposed algorithm can be improved by selecting the subcarrier with the least power per bit rather than the least power to upgrade a modulation

level to achieve the optimal solutions with current conditions. Moreover, we use the RA strategy in this thesis to have the maximum throughput with the constraints of total power and BER, but MA can also be considered for cases where the requirement is to find the minimum power to achieve a data rate and a target BER.

Appendix A
Average Symbol Energy in the Superposed Constellations

In this appendix, we elaborate on the average superposed symbol energy at the relay for different modulations used at the user sides. The first observation that we will make is that if there is no attenuation between the users and the relay the minimum distance between the symbols in the original constellation is the same as the minimum distance between the superposed symbols at the relay. The second observation is that the average energy of the superposed symbols is twice the energy of the original symbol constellations. The latter result is quite obvious as superposed symbols are the sum of two symbols from the original constellations where all original symbols are equiprobable. We corroborate this observation by performing more detailed analysis of the superposed symbols. Specifically, this is accomplished by analyzing the statistical distribution for the frequency of occurrence of different symbols in the superposed constellation. Based on these two observations, we conclude that the symbol error rate performance of the superposed constellations is 3dB worse than that of the original constellation at the user sides.

First, we show that the minimum distance between symbols is the same in the modulation constellation at users and in the modulation constellation at the relay, although the received symbols at the relay are two superposed symbols from users. Assuming the average symbol energy of transmitted symbols at users is equal to one despite modulation levels, the relationship between the modulation (BPSK, 4-QAM, 16-QAM and 64-QAM) at users and its corresponding received modulation at the relay is illustrated in the following figures. Each figure shows that the minimum distance between symbols in a modulation constellation for transmission is the same as the one in the corresponding modulation constellation at the relay.

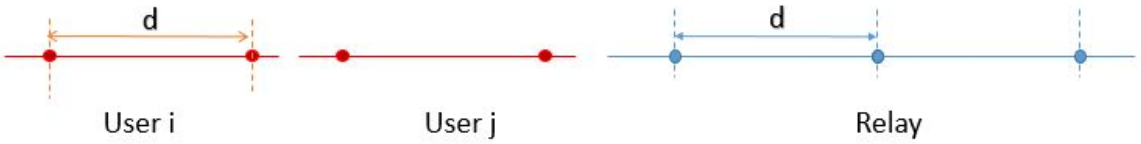

Figure A.1: The minimum distance between symbols in BPSK modulation used at users and in the corresponding ternary symbols at the relay.

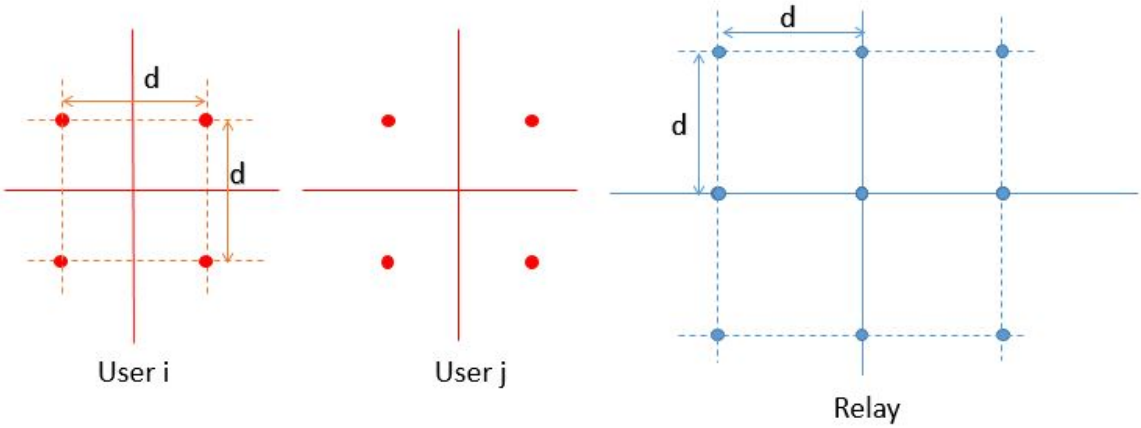

Figure A.2: The minimum distance between symbols in 4-QAM original constellation at users and in the corresponding superposed constellation at the relay.

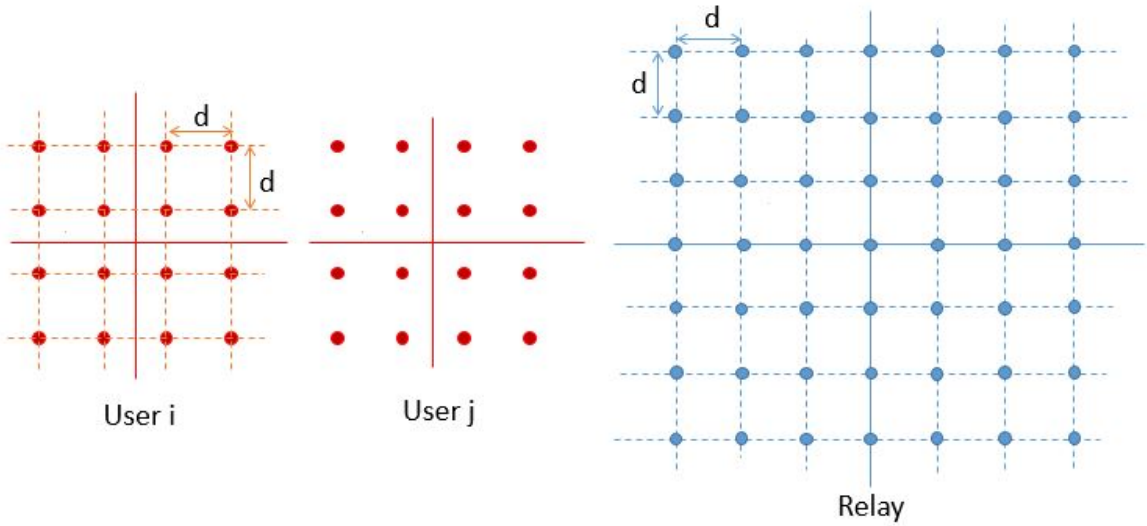

Figure A.3: The minimum distance between symbols in 16-QAM original constellation at users and in the superposed constellation at the relay.

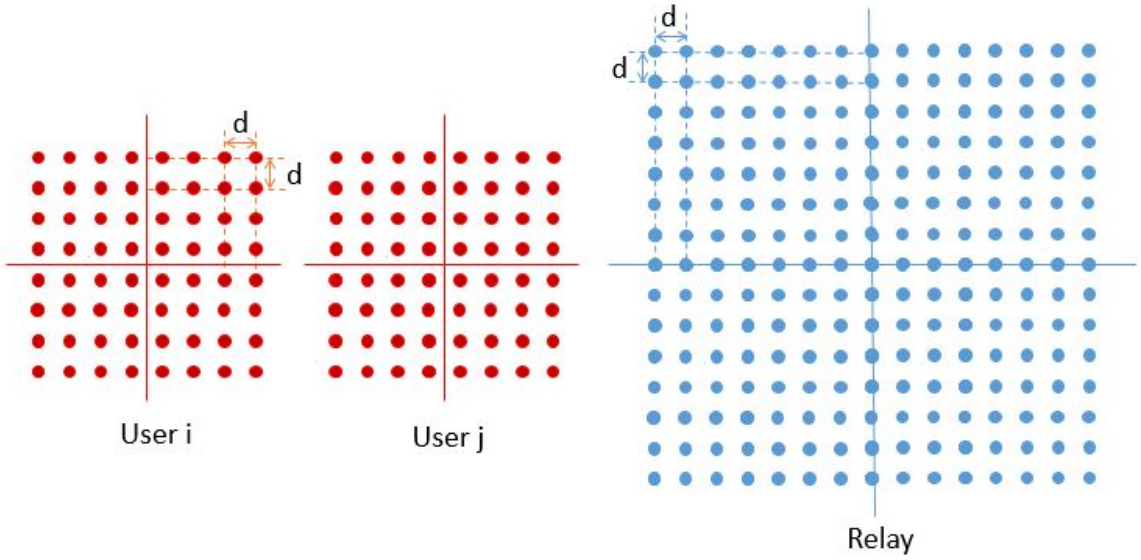

Figure A.4: The minimum distance between symbols in 64-QAM original constellation at users and in the superposed constellation at the relay.

Moreover, the average received symbol energy should be two because the received symbol is two superposed symbols whose average symbol energy is one. This can be proved by considering the frequency of occurrence of different superposed symbols and weighting correspondingly their energies. We take the original 4-QAM constellation as an example, and the probability of each received 9-QAM symbol at the relay in the superposed constellation is shown in Fig. A.5. Then the average received symbol at the relay can be calculated as:

$$\begin{aligned} E_{s,avg} &= 4 \times \frac{1}{16} \times \left\{ \left(\frac{2}{\sqrt{2}} \right)^2 + \left(\frac{2}{\sqrt{2}} \right)^2 \right\} + 4 \times \frac{1}{8} \times \left\{ \left(\frac{2}{\sqrt{2}} \right)^2 + 0 \right\} + 4 \times \frac{1}{4} \times 0 \\ &= 1 + 1 + 0 = 2 \end{aligned} \tag{A.1}$$

Through similar calculations for other modulation levels, we verified the same result that the average superposed symbol energy is twice the energy of the original constellations. In this way, the received symbols at the relay require twice of the energy of the original constellation to maintain the same minimum distance between symbols in the superposed constellation. This indicates that the BER performance of the received symbols is 3dB worse than that of the transmitted symbols at the user sides.

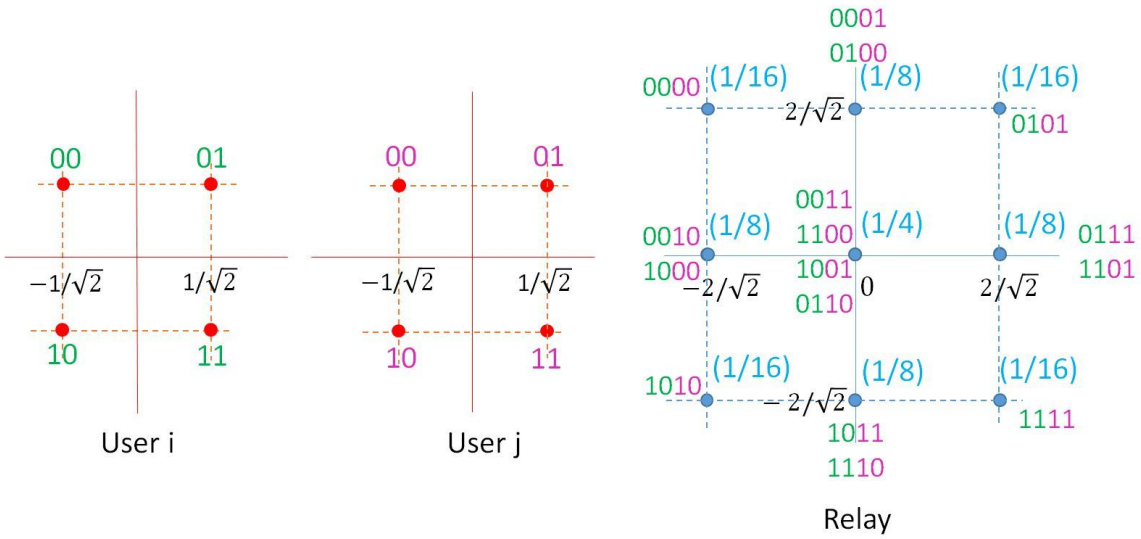

Figure A.5: The probability of superposed symbols at the relay when the equiprobable 4-QAM is deployed at the users.

Bibliography

[1] A. H. Mohammed, B. Dai, B. Huang, M. Azhar, G. Xu, P. Qin, and S. Yu, "A survey and tutorial of wireless relay network protocols based on network coding," *J. Network and Comput. Applicat.*, vol. 36, no. 2, pp. 593 – 610, 2013.

[2] O. El Ayach, S. W. Peters, and R. W. Heath, Jr, "The Practical Challenges of Interference Alignment," *ArXiv e-prints*, June 2012.

[3] A. Nosratinia, T. Hunter, and A. Hedayat, "Cooperative communication in wireless networks," *IEEE Commun. Mag.*, vol. 42, no. 10, pp. 74–80, Oct 2004.

[4] S.-Y. Li, R. Yeung, and N. Cai, "Linear network coding," *IEEE Trans. Inform. Theory*, vol. 49, no. 2, pp. 371–381, Feb 2003.

[5] Z. Shengli, S.-C. Liew, and P. P. K. Lam, "Physical Layer Network Coding," *ArXiv e-prints*, April 2007.

[6] S. Zhang and S. C. Liew, "Physical layer network coding with multiple antennas," in *2010 IEEE Wireless Commun. and Networking Conf.*, April 2010, pp. 1–6.

[7] S. Katti, S. Gollakota, and D. Katabi, "Embracing wireless interference: Analog network coding," *SIGCOMM Comput. Commun. Rev.*, vol. 37, no. 4, pp. 397–408, Aug. 2007.

[8] S. Katti, H. Rahul, W. Hu, D. Katabi, M. Medard, and J. Crowcroft, "XORs in the air: Practical wireless network coding," *IEEE/ACM Trans. Networking*, vol. 16, no. 3, pp. 497–510, June 2008.

[9] D. Gunduz, A. Goldsmith, and H. Poor, "MIMO two-way relay channel: Diversity-multiplexing tradeoff analysis," in *2008 Asilomar Conf. Signals, Syst. and Comput.*, Oct 2008, pp. 1474–1478.

[10] M. Medard and A. Sprintson, *Network Coding Fundamentals and Applications*. Academic Press, 2012.

[11] M. Maddah-Ali, A. Motahari, and A. Khandani, "Communication over MIMO X channels: Interference alignment, decomposition, and performance analysis," *IEEE Trans. Inform. Theory*, vol. 54, no. 8, pp. 3457–3470, Aug 2008.

[12] V. Cadambe and S. Jafar, "Interference alignment and degrees of freedom of the K user interference channel," *IEEE Trans. Inform. Theory*, vol. 54, no. 8, pp. 3425–3441, Aug 2008.

[13] S. Jafar and S. Shamai, "Degrees of freedom of the MIMO X channel," in *IEEE Global Telecommun. Conf.*, Nov 2007, pp. 1632–1636.

[14] N. Lee, J.-B. Lim, and J. Chun, "Degrees of freedom of the MIMO Y channel: Signal space alignment for network coding," *IEEE Trans. Inform. Theory*, vol. 56, no. 7, pp. 3332–3342, July 2010.

[15] G. Zheng, I. Krikidis, C. Masouros, S. Timotheou, D.-A. Toumpakaris, and Z. Ding, "Rethinking the role of interference in wireless networks," *IEEE Commun. Mag.*, vol. 52, no. 11, pp. 152–158, Nov 2014.

[16] N. Wang, Z. Ding, X. Dai, and A. Vasilakos, "On generalized MIMO Y channels: Precoding design, mapping, and diversity gain," *IEEE Trans. Veh. Technol.*, vol. 60, no. 7, pp. 3525–3532, Sept 2011.

[17] Y. Su, Y. Li, and J. Liu, "Amplify-and-Forward MIMO Y channel: Power allocation based signal space alignment," in *2012 IEEE Veh. Technol. Conf.*, Sept 2012, pp. 1–5.

[18] Z. Zhou and B. Vucetic, "An iterative beamforming optimization algorithm for generalized MIMO Y channels," in *2012 IEEE Int. Conf. Commun.*, June 2012, pp. 4595–4599.

[19] K. K. Teav, Z. Zhou, and B. Vucetic, "Performance optimization of MIMO Y channels: Interference alignment and signal detection," *IEEE Communications Letters*, vol. 18, no. 1, pp. 66–69, January 2014.

[20] Z. Zhou, "Enhancing Signal Alignment in MIMO Y Channels with Space and Time Scheduling," Master's thesis, Dalhousie University, Halifax, 2015, [Online]: http:dalspace.library.dal.ca/handle/10222/64675.

[21] R. F. H. Fischer and J. B. Huber, "A new loading algorithm for discrete multitone transmission," in *Global Telecommunications Conference, 1996. GLOBECOM '96. 'Communications: The Key to Global Prosperity*, vol. 1, Nov 1996, pp. 724–728 vol.1.

[22] N. U. Hassan and M. Assaad, "Low complexity margin adaptive resource allocation in downlink MIMO-OFDMA system," *IEEE Transactions on Wireless Communications*, vol. 8, no. 7, pp. 3365–3371, July 2009.

[23] B. Gui and L. J. Cimini, "Bit loading algorithms for cooperative OFDM systems," in *MILCOM 2007 - IEEE Military Communications Conference*, Oct 2007, pp. 1–7.

[24] K. S. Al-Mawali, A. Z. Sadik, and Z. M. Hussain, "Simple discrete bit-loading for OFDM systems in power line communications," in *Power Line Communications and Its Applications (ISPLC), 2011 IEEE International Symposium on*, April 2011, pp. 267–270.

[25] J. Yang, I. Koo, Y. Choi, and K. Kim, "A dynamic resource allocation scheme to maximize throughput in a multimedia CDMA system," in *Vehicular Technology Conference, 1999. VTC 1999 - Fall. IEEE VTS 50th*, vol. 1, 1999, pp. 348–351 vol.1.

[26] G. V. Klimovitch and J. M. Cioffi, "Maximizing data rate-sum over vector multiple access channel," in *Wireless Communications and Networking Confernce, 2000. WCNC. 2000 IEEE*, vol. 1, 2000, pp. 287–292 vol.1.

[27] C. E. Shannon, "A mathematical theory of communication," *The Bell System Technical Journal*, vol. 27, no. 4, pp. 623–656, Oct 1948.

[28] D. Tse and P. Viswanath, *Fundamentals of Wireless Communication*. New York, NY, USA: Cambridge University Press, 2005.

[29] D. P. Palomar and J. R. Fonollosa, "Practical algorithms for a family of waterfilling solutions," *IEEE Transactions on Signal Processing*, vol. 53, no. 2, pp. 686–695, Feb 2005.

[30] A. Goldsmith, *Wireless Communications*. New York: Cambridge University Press, 2005.

[31] Y. G. Li, *Orthogonal Frequency Division Multiplexing for Wireless Communications*. Berlin, Heidelberg: Springer-Verlag, 2009.

[32] V. Kuhn, *Wireless Communications over MIMO Channels: Applications to CDMA And Multiple Antenna Systems*. John Wiley & Sons, 2006.

[33] D. Hughes-Hartogs, "Ensemble modem structure for imperfect transmission media," Mar. 15 1988, uS Patent 4,731,816. [Online]. Available: http://www.google.com/patents/US4731816

[34] P. S. Chow, J. M. Cioffi, and J. A. C. Bingham, "A practical discrete multitone transceiver loading algorithm for data transmission over spectrally shaped channels," *IEEE Transactions on Communications*, vol. 43, no. 2/3/4, pp. 773–775, Feb 1995.

[35] Q. Yu and Y. Wang, "Improved chow algorithm used in adaptive OFDM system," in *Communications and Mobile Computing (CMC), 2010 International Conference on*, vol. 2, April 2010, pp. 430–432.

[36] W. Yang, Y. Li, X. Yu, and Y. Sun, "The antenna selection strategy of MIMO Y channel and performance analysis," in *Communications in China (ICCC), 2014 IEEE/CIC International Conference on*, Oct 2014, pp. 479–484.

[37] V. Namboodiri, K. Venugopal, and B. S. Rajan, "Physical layer network coding for two-way relaying with QAM," *IEEE Transactions on Wireless Communications*, vol. 12, no. 10, pp. 5074–5086, October 2013.

[38] F. Wang, Q. Song, S. Wang, and L. Guo, "Rate and power adaptation for physical-layer network coding with M-QAM modulation," in *2014 IEEE International Conference on Communications (ICC)*, June 2014, pp. 5508–5513.

[39] K. K. Teav, Z. Zhou, and B. Vucetic, "Throughput optimization for MIMO Y channels with physical network coding and adaptive modulation," in *Vehicular Technology Conference (VTC Spring), 2012 IEEE 75th*, May 2012, pp. 1–5.

[40] S. Wang, Q. Song, L. Guo, and A. Jamalipour, "Constellation mapping for physical-layer network coding with M-QAM modulation," in *Global Communications Conference (GLOBECOM), 2012 IEEE*, Dec 2012, pp. 4429–4434.

[41] K. Hassan and W. Henkel, "Fast prioritized bit-loading and subcarriers allocation for multicarrier systems," in *Vehicular Technology Conference (VTC 2010-Spring), 2010 IEEE 71st*, May 2010, pp. 1–5.

[42] O. El Ayach, S. Peters, and R. Heath, "The feasibility of interference alignment over measured MIMO-OFDM channels," *IEEE Trans. Vehicular Technol.*, vol. 59, no. 9, pp. 4309–4321, Nov 2010.

[43] P. Aquilina and T. Ratnarajah, "Performance analysis of IA techniques in the MIMO IBC with imperfect CSI," *IEEE Transactions on Communications*, vol. 63, no. 4, pp. 1259–1270, April 2015.

[44] X. Chen and C. Yuen, "On interference alignment with imperfect CSI: Characterizations of outage probability, ergodic rate and SER," *IEEE Transactions on Vehicular Technology*, vol. 65, no. 1, pp. 47–58, Jan 2016.

[45] X. Yin, X. Yu, Y. Liu, W. Tan, and X. Chen, "Performance analysis of multiuser MIMO system with adaptive modulation and imperfect CSI," in *Information and Communications Technologies (IETICT 2013), IET International Conference on*, April 2013, pp. 571–576.